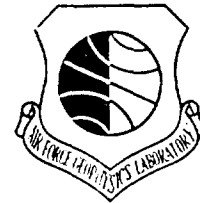


# LEVEL

①

AFGL-TR-80-0186  
ENVIRONMENTAL RESEARCH PAPERS, NO. 707



## A One-Dimensional Vertical Diffusion Parameter for Extremely Inhomogeneous, Layered Turbulence in Stratified Fluids

EDMOND M. DEWAN

16 June 1980

STIC  
OCT 16 1980  
C

Approved for public release; distribution unlimited.

AERONOMY DIVISION PROJECT 6687  
**AIR FORCE GEOPHYSICS LABORATORY**  
HANSCOM AFB, MASSACHUSETTS 01731

**AIR FORCE SYSTEMS COMMAND, USAF**



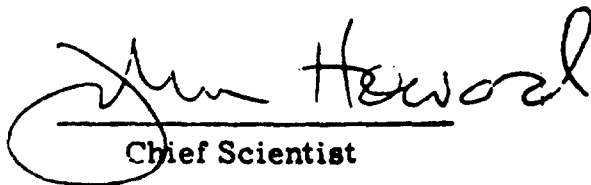
AD A090340

DDC FILE COPY

This report has been reviewed by the ESD Information Office (OI) and is releasable to the National Technical Information Service (NTIS).

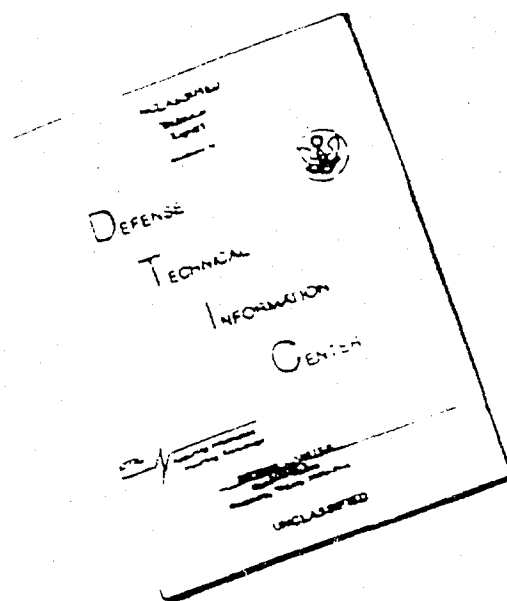
This technical report has been reviewed and is approved for publication.

FOR THE COMMANDER

  
Chief Scientist

Qualified requestors may obtain additional copies from the Defense Technical Information Center. All others should apply to the National Technical Information Service.

# DISCLAIMER NOTICE



THIS DOCUMENT IS BEST QUALITY AVAILABLE. THE COPY FURNISHED TO DTIC CONTAINED A SIGNIFICANT NUMBER OF PAGES WHICH DO NOT REPRODUCE LEGIBLY.

(14) AFGL-TR-80-0186  
AFGL-ERP-707

Unclassified SECURITY CLASSIFICATION OF THIS PAGE (When Data Entered)		
REPORT DOCUMENTATION PAGE		READ INSTRUCTIONS BEFORE COMPLETING FORM
1. REPORT NUMBER AFGL-TR-80-0186	2. GOVT ACCESSION NO. AD-A090340	3. RECIPIENT'S CATALOG NUMBER
4. TITLE (and Subtitle) A ONE-DIMENSIONAL VERTICAL DIFFUSION PARAMETER FOR EXTREMELY INHOMOGENEOUS, LAYERED TURBULENCE IN STRATIFIED FLUIDS.		5. TYPE OF REPORT & PERIOD COVERED Scientific, Interim.
6. AUTHOR(s) Edmond M. Dewan		7. PERFORMING ORG. REPORT NUMBER ERP No. 707
8. PERFORMING ORGANIZATION NAME AND ADDRESS Air Force Geophysics Laboratory (LKD) Hanscom AFB Massachusetts 01731		9. CONTRACT OR GRANT NUMBER(s)
10. CONTROLLING OFFICE NAME AND ADDRESS Air Force Geophysics Laboratory (LKD) Hanscom AFB Massachusetts 01731		11. PROGRAM ELEMENT, PROJECT, TASK AREA & WORK UNIT NUMBERS 62101F 68870506
12. MONITORING AGENCY NAME & ADDRESS (if different from Controlling Office) 1052		13. DATE 18 June 1980
		14. NUMBER OF PAGES 51
		15. SECURITY CLASS. (of this report) Unclassified
		16. DECLASSIFICATION/DOWNGRADING SCHEDULE
17. DISTRIBUTION STATEMENT (of this Report) Approved for public release; distribution unlimited.		
18. DISTRIBUTION STATEMENT (of the abstract entered in Block 20, if different from Report)		
19. SUPPLEMENTARY NOTES		
20. KEY WORDS (Continue on reverse side if necessary and identify by block number) Turbulence      Fluid dynamics      Environment Transport      Ocean Stratosphere      Dynamics Pollution      Meteorology Diffusion      Differential equations		
21. ABSTRACT (Continue on reverse side if necessary and identify by block number) A self-consistent method of characterizing vertical turbulent transport by means of a diffusion parameter is demonstrated for the extremely inhomogeneous case of layered turbulence in a stratified fluid. Between the horizontal turbulent layers, horizontal laminar flow is assumed to occur, and molecular diffusion is ignored. The layers are assumed to occur at random heights with random thickness. An analogy is made between the process of random mixing layers and the finite difference representation of the diffusion		

DD FORM 1 JAN 73 1473 EDITION OF 1 NOV 68 IS OBSOLETE

Unclassified  
SECURITY CLASSIFICATION OF THIS PAGE (When Data Entered)


409578 JLM

Unclassified

SECURITY CLASSIFICATION OF THIS PAGE(When Data Entered)

~~20.~~ Abstract (Continued).

equation. It is demonstrated by means of a series of digital computer experiments that, in the case where total mixing takes place within the turbulent layers, the diffusion parameter herein developed is the valid one to use (in contrast to "eddy diffusivity"). The relation between this inhomogeneous diffusion parameter and practical experimental measurements is given. The motive behind this investigation involves vertical transport of pollution in the environment in general and in the stratosphere in particular.



Unclassified

SECURITY CLASSIFICATION OF THIS PAGE(When Data Entered)

## Preface

The present formulation is based in part on published and unpublished work done with N. W. Rosenberg in 1975. I also wish to acknowledge help from Neal Grossbard, not only for his programming, but for his "boundary condition free" technique used in this report to calculate  $K_B$ -FLUX. I also acknowledge suggestions from Dr. C. Stergis, Dr. T. Van Zandt, Dr. A. Quesada, J. Brown, and Dr. J. O'Brien.

Accession For	
NTIS GRA&I	<input checked="" type="checkbox"/>
DTIC TAB	<input type="checkbox"/>
Unannounced	<input type="checkbox"/>
Justification	
By _____	
Distribution/	
Availability Codes	
Dist	Avail and/or Special
<b>A</b>	

## Contents

1. INTRODUCTION	7
1.1 Assumptions and Definition of "Bulk Diffusivity"	8
2. THE MECHANISM OF TRANSPORT BY MIXING LAYERS	10
3. RANDOM MIXING AS A STOCHASTIC STIMULATION OF THE DIFFUSION EQUATION	12
4. SIMULATION PROGRAM FOR $K_B = F/(\partial \bar{\phi}/\partial z)$	15
5. CALCULATION OF $K_B$ FROM DIFFUSIVE EFFECTS	20
5.1 Delta Function	20
5.2 Intrusion from Boundaries	22
5.3 Insulated Slab-Initially Linear $\phi(z, 0)$	24
6. CONNECTIONS OF CERTAIN PARAMETER VALUES TO EXPERIMENTAL DATA, AND SIMULATIONS OF MIXING LAYER TRANSPORT	26
6.1 Relations Between Parameters $\Delta t$ and $\Lambda$ and Possible Measurements	26
6.2 Simulation Results	28
6.2.1 $K_B$ -FLUX	28
6.2.2 $K_B$ -DELTA	33
6.2.3 $K_B$ -INTR	37
6.2.4 $K_B$ -INSUL	40
6.2.5 $K_B$ -CALC	44
6.3 Summary of Simulation Results	44
7. SUMMARY AND CONCLUSIONS	45

## Contents

REFERENCES	47
APPENDIX - Continuous Estimate of Amount of Material Per Unit Area Passing Through Bottom of "Slab" Due to an Average Mixing Event and Modification of the Estimate of $K_B$ -CALC	49

## Illustrations

1. Single Stationary Mixing Layer Within a Slab of Atmosphere	11
2. Mechanism of Vertical Transport by Sequence of Overlapping Mixing Layers in the Presence of a Gradient	11
3. A "Mixing Layer Simulation" of the Finite Difference Diffusion Equation	13
4. Schematic Representation for Simulation of Vertical Transport Through a Slab and the Techniques for Avoidance of Boundary Conditions	16
5. Explanation of the Calculation of $K_B$ by Means of Flux Out of the Bottom of the Slab by Means of a "Mix-Through" Process	19
6. Schematic Drawing of Delta Function Diffusion Expected from Continuous Theory	21
7. Expected Behavior of Diffusion Through Boundaries in Continuous Theory of Diffusion	23
8. Expected Behavior of Temperature Inside an Insulated Slab with Initially Linear Temperature Profile	25
9. Bulk Diffusivity, $K_B$ (as Calculated in the Simulation Via the Flux) as a Function of Time	28
10. Simulated Evolution of Delta Function When Exposed to Random Mixing Layers	33
11. Simulated Evolution of the Case of Infinitely Conducting Walls and Diffusion Inwards by Means of Random-Mixing Layers	38
12. Simulated Evolution of "Insulated Slab" Case Via Random-Mixing Layers	41

## Tables

1. Distribution of Layer Thicknesses, $\Delta$	17
2. Diffusion Parameter, $K_B$ , for Various Cases	45



## A One-Dimensional Vertical Diffusion Parameter for Extremely Inhomogeneous, Layered Turbulence in Stratified Fluids

### 1. INTRODUCTION

The main motivation for this investigation is the present concern about stratospheric pollution. The stratosphere is characterized by a high degree of stability, and turbulence in this region occurs in the form of thin, random, horizontal, pancake-shaped layers.<sup>1</sup> The shear, or Kelvin-Helmholtz, instability is presumed to be the mechanism for the formation of these layers. The nature of this type of turbulence is discussed in Rosenberg and Dewan,<sup>1</sup> Dewan (1979a),<sup>2</sup> and Dewan (1979b).<sup>3</sup> There are two purposes for the present report. The first is to overcome some of the initial criticisms we received (Rosenberg and Dewan<sup>1</sup>) due to the fact that we used the term "eddy diffusivity." As will be seen, we will be considering an entirely new parameter which is, in a sense, completely different from the usual eddy diffusion. This new parameter, like eddy diffusion, is phenomenological in nature; however, this is where the similarity ends. To explain the new parameter, this report shall make use of an analogy between the random layer mixing

---

(Received for publication 13 June 1980)

1. Rosenberg, N.W. and Dewan, E.M. (1975) Stratospheric Turbulence and Vertical Effective Diffusion Coefficient, AFGL-TR-75-0519, AD A019 701.
2. Dewan, E.M. (1979a) Estimates of Vertical Eddy Diffusion Due to Turbulent Layers in the Stratosphere, AFGL-TR-79-0042, AD A069 750.
3. Dewan, E.M. (1979b) Mixing in Below Turbulence and Stratospheric Eddy Diffusion, AFGL-TR-79-0091, AD A074 466.

process mentioned above and the finite difference formalism used to numerically simulate the diffusion equation. That such an analogy exists may surprise some readers; nevertheless, it represents a good way to convey the physics of the process. This report's second purpose is to demonstrate that our new parameter is indeed a self-consistent, "diffusion like" parameter. This will be achieved by means of a series of digital computer simulations.

The usual eddy diffusion parameter (eddy diffusion coefficient) for turbulence transport assumes that, at least as a practical approximation, the turbulence is essentially homogeneous in some sense. Pasquill<sup>4</sup> defines eddy diffusivity,  $K$ , as

$$K = v l \quad (1)$$

where  $v$  and  $l$  are the velocity and size scale lengths, respectively, which are appropriate for the turbulence in question. Another form to be found in the literature (Lilly et al,<sup>5</sup> Panofsky and Heck<sup>6</sup>) is

$$K = \frac{\bar{\epsilon}}{3N_B^2} \quad (2)$$

where  $\bar{\epsilon}$  is the average eddy dissipation rate and  $N_B$  is the buoyancy frequency.

#### 1.1 Assumptions and Definition of "Bulk Diffusivity"

We shall assume that (a) the turbulent layers occur at random heights and at random times (this assumption is usually made in the context of stable fluids, see for example, Panofsky and Heck,<sup>6</sup> Lilly et al,<sup>5</sup> Woods,<sup>7</sup> and Woods and Wiley<sup>8</sup>), (b) there is no vertical transport outside of the turbulent layers (in other words, between layers, motion is regarded as laminar), and (c) within the mixing layers, the mixing is presumed to be total. Regarding this last assumption, it remains to be proven correct; on the other hand, certain experimental observations

4. Pasquill, F. (1974) Atmospheric Diffusion, 2nd Ed., John Wiley & Sons.
5. Lilly, D.K., Waco, D.E., and Adelfang, S.I. (1975) Stratospheric mixing estimated from high altitude turbulence measurements by using energy budget techniques, The Natural Stratosphere of 1974, CIAP Monograph 1, Final Report, DOT-TST-75-51, pp. 8-81 to 8-90.
6. Panofsky, H.A. and Heck, W. (1975) Stratospheric mixing estimates from heat flux measurements, The Natural Stratosphere of 1974, CIAP Monograph 1, DOT-TST-75-51, pp. 8-90 to 8-92.
7. Woods, J.D. (1968) Wave-induced shear instability in the summer thermocline, J. Fluid Mech. 32:791-800.
8. Woods, J.D. and Wiley, R.L. (1972) Billow turbulence and ocean microstructure, Deep Sea Research and Oceanic Abstr. 19:87-121.

have been made which are consistent with it. These are the temperature-profile studies of Mantis and Peppin,<sup>9</sup> who note that balloon-borne sensors indicate that in the lower stratosphere and upper troposphere there are regions of nearly adiabatic lapse rates. Analogously, in the upper ocean where the stability situation is very much like the stratosphere, Woods and Wiley<sup>8</sup> have reported step-like structures in the vertical temperature profiles. Such profiles are consistent with the hypothesis that total mixing can result from the turbulent layers. Finally, one more assumption is needed: (d) there is enough horizontal homogeneity so that a one-dimensional vertical transport model will be adequate.

In the next section, the mechanism for vertical transport by means of random mixing layers will be explained. At this stage, however, the assumption that total mixing takes place can be used to suggest (by means of a dimensional argument) that any effective "bulk diffusion coefficient," which parameterizes layered turbulence, could not be appropriately described by Eqs. (1) or (2). The argument is based on the fact that the width of the layer and the time intervals between layer formations would determine the transport. These parameters do not explicitly appear in Eqs. (1) or (2), and unless there were a proven connection, say, between  $N_B$  and the time interval between new random layer profiles, it is not at all clear that Eqs. (1) or (2) could be useful in the present context. On the other hand, the parameter to be developed here will explicitly depend on layer thickness,  $\Lambda$ , and the relevant time interval,  $\Delta t$ .

Before proceeding further, it is essential to precisely define  $K_B$ , the bulk vertical diffusivity parameter. Let  $\bar{F}$  designate the average flux of material through a given slab of stable fluid. This slab is assumed to be very much larger than the largest turbulent layers. Let  $\phi$  designate a scalar quantity, such as potential temperature or mixing ratio of some neutrally buoyant substance (for example, pollutant). Then

$$K_B = \frac{\bar{F}}{\partial \phi / \partial z} \quad (3)$$

where the overbar designates an average. This definition is based on Fourier's heat transport equation (cf. Dewan<sup>2</sup> as well as Panofsky and Heck<sup>6</sup>).

---

9. Mantis, M. T. and Peppin, T. J. (1971) Vertical temperature structure of the free atmosphere at mesoscale, J. Geophys. Res. 20:8621-8628.

## 2. THE MECHANISM OF TRANSPORT BY MIXING LAYERS

Figure 1 depicts a slab of stable atmosphere, and within the slab is located a single turbulent layer. As previously mentioned, we assume that no vertical transport exists outside of such a turbulent layer, but let us temporarily add one more assumption: (e) the layer remains fixed at one altitude. We ask the question: "What is the flux,  $F$ , between points Y and Z, located at the top and bottom of the slab, respectively?" Obviously, there will be no transport of material from point Y to Z. Equation (3) therefore implies  $K_B = 0$ , since there  $F$  is to be interpreted as a flux from point Y to point Z. We have an analogy here with the situation in which there is an electrical conductor located between two regions of insulation. One cannot average the conductivity of the "sandwich." One is left with a nonconductor (in the vertical), no matter how low the resistance of the conductor inside may be. These considerations imply that the intensity of turbulence (once total mixing is assumed) is of no direct relevance, and that, as will be made more clear below, the temporal behavior of the layers is absolutely crucial for transport effects.

Next consider Figure 2. Here we consider a temporal sequence of layer formation. Layer I is the first to form. Total mixing takes place, and then the turbulence decays in time. Due to the gradient of  $\phi$  which is indicated, the mixing causes material in the upper half (A) of the layer to move into the lower half (B) of the layer. Next, imagine Layer II to form, and notice that Layer II significantly overlaps the original position taken previously by I. When II has mixed, the profile of  $\phi(z)$  would again be altered to a single average value within the layer. This is due to the assumption of total mixing. This process would result in a further net transfer of  $\phi$  (for example, material) downward. It should be clear that some material which was initially near the top of Layer I (for example, in region A) can find its way, at the end of this two-fold mixing process, to a point near the bottom of Layer II. This simple example demonstrates the essential mechanism for vertical transport by means of a random sequence of mixing layers in an otherwise stable fluid (all other flow being laminar and horizontal). Such a process can eventually give a net flux from the top to the bottom of the slab. Notice that there are two conditions needed for the mechanism to function: (a) a large amount of mixing within the layer, and (b) an overlap of layer positions.

After the random formation of turbulent layers in the above fashion, one could calculate an average flux  $\bar{F}$  across the slab, as well as  $\partial\bar{\phi}/\partial z$ .  $K_B$  could then be calculated from Eq. (3). In Rosenberg and Dewan<sup>1</sup> and Dewan,<sup>2</sup> it was shown that one can calculate an estimate for  $K_B$  (designated here as  $K_{B-CALC}$ ) if one assumes, among other things, a steady state. This will be discussed in the Appendix. The result is

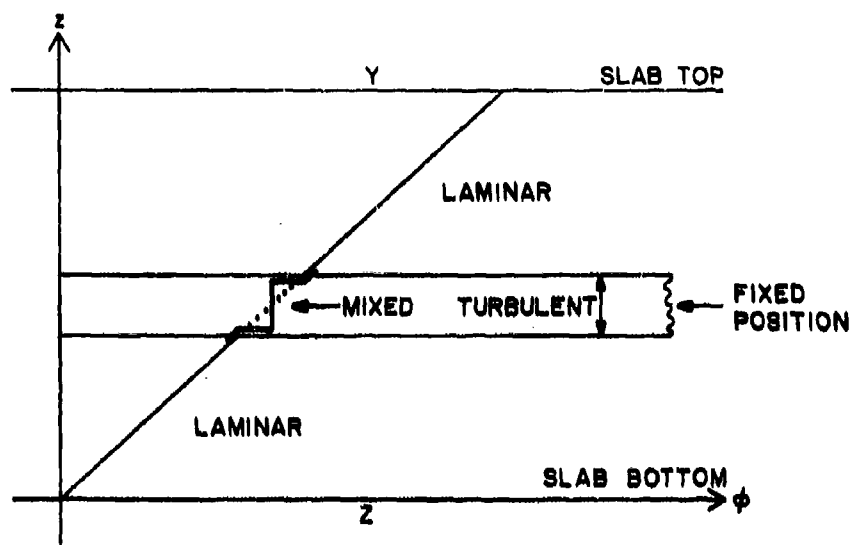


Figure 1. Single Stationary Mixing Layer Within a Slab of Atmosphere. No transport in this case

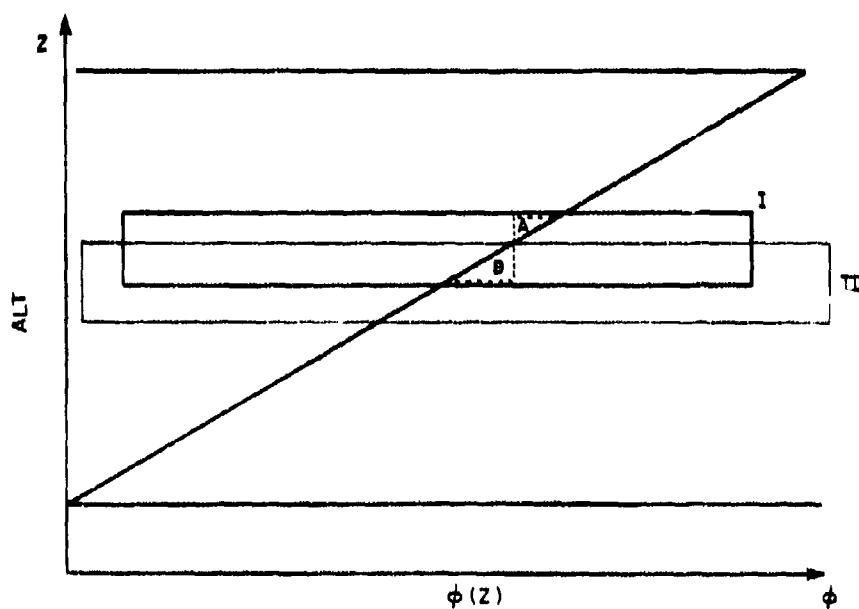


Figure 2. Mechanism of Vertical Transport by Sequence of Overlapping Mixing Layers in the Presence of a Gradient

$$K_{B-CALC} = \frac{(\overline{\Lambda/2})^2}{2\Delta t_b} \quad (4)$$

where  $\Lambda$  is layer thickness, the overbar is an average, and  $\Delta t_b$  is the average time interval between layer formations overlapping the bottom boundary of the slab (or any preset altitude, for that matter). Equation (4) is based on Eq. (3).

### 3. RANDOM MIXING AS A STOCHASTIC STIMULATION OF THE DIFFUSION EQUATION

The diffusivity given by Eq. (4) is new (as of Rosenberg and Dewan<sup>1</sup>), and before it can be fully accepted as valid, it must be shown to be self-consistent. In other words, the question remains as to whether or not random mixing layer transport, as estimated from Eq. (4), is diffusive in nature in the sense that one could use the same  $K_B$  to describe the transport effects on any initial distribution of  $\phi(z)$ . In addition, it is essential to establish  $K_B$  on a more reliable physical/mathematical basis than has been done heretofore. The remainder of this paper will be devoted to these objectives, and the purpose of the present section is to connect the random mixing layer process to the finite difference formulation of the diffusion equation. (This analogy was mentioned previously in the introduction.)

It is well known that if one wishes to simulate a Laplacian,  $\nabla^2\psi$ , by means of a finite-difference numerical scheme, one averages a given lattice point with all of its nearest neighbors, and replaces the original value at the given lattice point with this average. This process is repeated for each time step. Now consider the effect of a mixing layer. In effect, the layer averages the values of  $\phi(z)$  within its boundaries and replaces these original values with the average (see Figures 1 and 2). This leads to the idea that random turbulent layers in a stable fluid could stochastically simulate the one-dimensional diffusion equation.

In order to make this idea more concrete, we first consider a specific pattern of a mixing layer sequence which results in an exact simulation of the finite difference diffusion equation. This pattern will, of course, be extremely regular, and in this respect, will differ from the random situation postulated for stratified turbulence. Nevertheless, it will serve to establish an important connection between the two processes.

Figure 3 shows, in epoch 1, a vertical set of layers, each in sequence immediately above the other. They nearly touch, but there is no overlap. These are to be imagined as mixing until all pairs of altitude points are averaged (we assume each layer contains two altitude grid points). In principle, these layers would not have to mix simultaneously. We assume, however, that the mixing process has

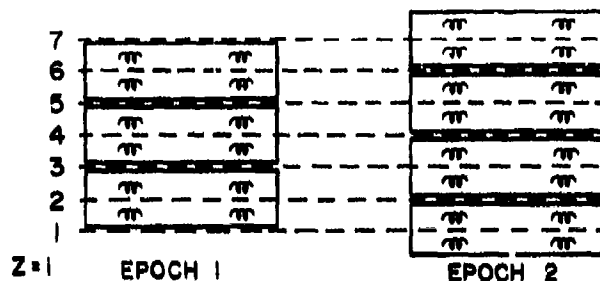


Figure 3. A "Mixing Layer Simulation" of the Finite Difference Diffusion Equation

terminated at a specific time which designates the end of Epoch 1. After this, the original layers are replaced by a different set of layers (Time 2 in Figure 3), which precisely and symmetrically overlap the positions of the original layers. In other words, the "cracks" between the original layer boundaries are now in the exact centers of the Epoch 2 layers. These layers then mix and perform another averaging of altitude pairs.

The above double sequence is then repeated for each time step, and so on. We now calculate its effects. Let  $z$ , as usual, designate the altitude, and let  $\Delta z$  be the distance between the vertical points. Let  $t$  designate the time, and let  $\Delta t$  be the interval of time between steps. Each epoch described above corresponds to only one-half of a time step,  $\Delta t/2$ . Thus, for  $\phi$ , at the end of Epoch 1, we have

$$\phi\left(t + \frac{\Delta t}{2}, z\right) = \frac{\phi(t, z) + \phi(t, z + \Delta z)}{2} \quad (5)$$

In other words,  $\phi$  at  $z$ , at the end of the first epoch, equals the average of  $\phi$  taken at  $z$  and  $z + \Delta z$ . The mixing layer includes both  $z$  and  $z + \Delta z$ , the point  $z$  being located a distance  $(1/2)(\Delta z)$  from the bottom of the layer, while  $(z + \Delta z)$  would be  $(3/2)(\Delta z)$  up from the bottom (layer thickness =  $2 \Delta z$ ). Next, Epoch 2 of the time step (Epoch 2 in Figure 3) results in

$$\phi(t + \Delta t, z) = \frac{\phi\left(t + \frac{\Delta t}{2}, z\right) + \phi\left(t + \frac{\Delta t}{2}, z - \Delta z\right)}{2} \quad (6)$$

In other words, this time the average, or mixing, involves the grid point immediately below  $z$  (for example,  $z - \Delta z$ ). We now wish to relate  $\phi(t + \Delta t, z)$  to the original values of  $\phi$  at  $t$ . Therefore, insert Eq. (5)\* into Eq. (6) to obtain

$$\phi(t + \Delta t, z) = \frac{1}{4} [2\phi(t, z) + \phi(t, z + \Delta z) + \phi(t, z - \Delta z)] \quad (7)$$

Next, we put Eq. (7) into the form of the finite difference equation as follows: first, the finite time derivative will be defined by

$$\frac{\Delta \phi(z, t)}{\Delta t} = \frac{\phi(t + \Delta t, z) - \phi(t, z)}{\Delta t} \quad (8)$$

and the second spatial derivative (see any book on numerical analysis) will be defined

$$\frac{\Delta^2 \phi(t, z)}{\Delta z^2} = \frac{\phi(t, z + \Delta z) - 2\phi(t, z) + \phi(t, z - \Delta z)}{\Delta z^2} \quad (9)$$

Finally, we define  $K$  as

$$K = \frac{1}{4} \frac{(\Delta z)^2}{\Delta t} \quad (10)$$

Rearranging Eq. (7), and using Eqs. (8), (9) and (10), we obtain

$$\frac{\Delta \phi}{\Delta t} = K \frac{\Delta^2 \phi}{(\Delta z)^2} \quad (11)$$

which is, of course, the finite difference diffusion equation. (Note the resemblance between Eqs. (10) and (4).) Thus, the sequence in Figure 3 exactly simulates Eq. (11). Actually, there are many more sequences which would effectively do the same thing, and the uniqueness of the process in Figure 3 is merely its simplicity.

The above discussion carries an important message; namely, that in spite of the extremely inhomogeneous and discrete nature of the process, a "diffusion" parameter, called  $K$  above, has an "exact" connection with the process of diffusion. Layered turbulence is extremely inhomogeneous in the vertical direction. It is difficult to imagine a form of turbulence which is more inhomogeneous in this

\*Equation (5) must be modified so that it can be used to be substituted into both terms in the numerator of Eq. (6).



respect. Nevertheless, we find here a way to meaningfully assign a diffusivity to the process.

As was mentioned, layered turbulence in actual fluids would differ from the above process by virtue of its stochastic nature: layers would presumably form at random altitudes, at random times and with random thickness. This leads to the next question. Could such a random process effectively simulate diffusion in a manner analogous to the above? Also, would it do so in a consistent manner?

In order to show that the answers to the above questions are affirmative, we shall make several digital simulations of the stochastic mixing process. The effective values of  $K_B$  will be determined directly from the simulated results by means of a comparison with continuous diffusion theory. We shall see that (a) the behavior of  $\phi(z)$  in time is extremely similar to the predictions of continuous theory, and (b) the  $K_B$  values inferred from the behavior of the simulations are in surprisingly accurate quantitative agreement with one another.

#### 4. SIMULATION PROGRAM FOR $K_B = \bar{F}/(\partial\phi/\partial z)$

In the following, a digital program for simulating the effects of random mixing layers will be described. More specifically, a program for ascertaining the value of  $K_B$  on the basis of Eq. (3) (see this section title) will be discussed in some detail. With minor modifications, the same program also provides the simulations to be given in Section 6. At the first reading, some readers may wish to skip some of the details.

Figure 4 shows the essential aspects of how the simulation was done. A "slab" of thickness  $R$  is depicted in an "environment" ( $z = 0$  to  $z = \max$ ). This slab could, for example, represent the entire stratosphere or upper ocean, or it could represent a smaller height region of interest. It is the region for which we seek a bulk value of diffusivity. The reason for the "environment" will be explained below. Inside the slab is a "turbulent" layer of random thickness  $\Lambda$  (at random altitude,  $z$ ), and within such a layer, the values of  $\phi$  would be replaced by the average value within the layer. The initial value of  $\phi$  is shown, and it is a straight line with  $\phi$  differing by unity in going from the bottom,  $B$ , to the top,  $A$ , of the slab. In other words, the slope of  $\phi$  across the slab is  $(1/R)$ , as shown; the same slope continues throughout the slab's "environment".

The height  $z$  is chosen by means of a random-number generator. As for the thickness,  $\Lambda$ , the following procedure was used. A second random number generator (which was independent from the one used for  $z$ ) was used to pick numbers from 0 to 99. The possible thicknesses of layers were  $3\Delta z$ ,  $5\Delta z$ ,  $7\Delta z$ ,  $9\Delta z$  and  $11\Delta z$ , that is, the layers were to contain from 3 to 11 points (odd only), and in the

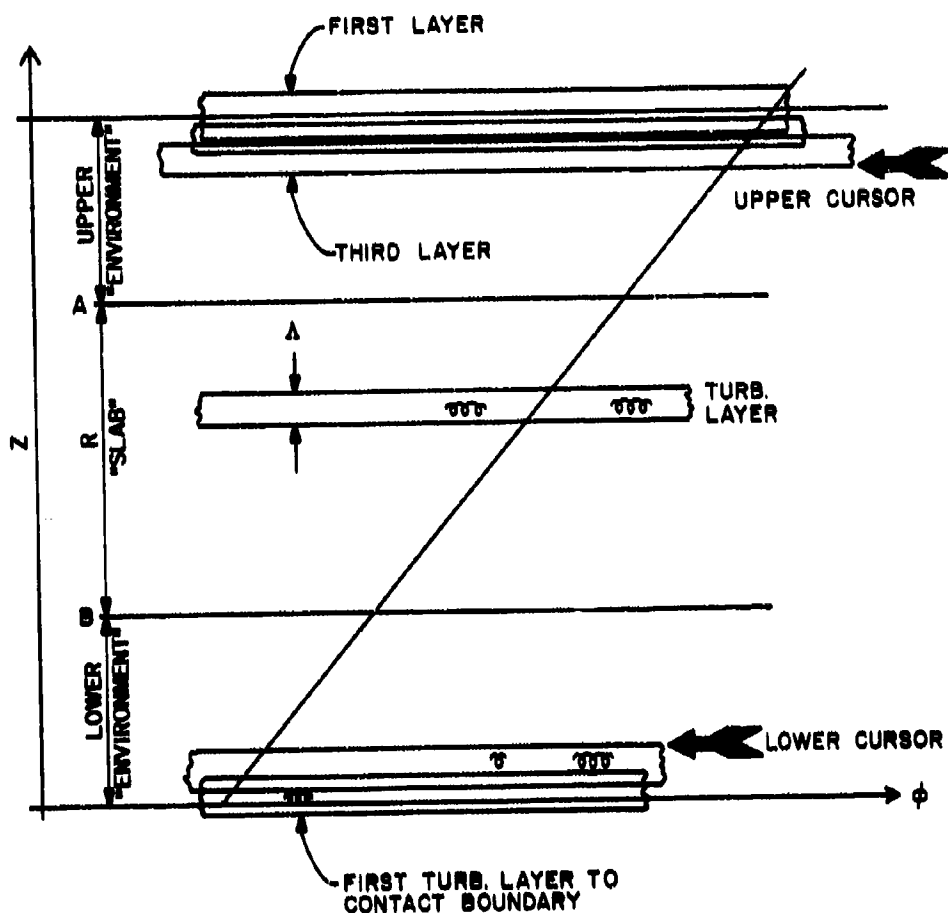


Figure 4. Schematic Representation for Simulation of Vertical Transport Through a Slab and the Techniques for Avoidance of Boundary Conditions

calculations  $\Delta z = 50$  m. The use of odd integers made it possible to have an unambiguous center point, and it was this center point that was placed at the point  $z$  previously selected. The mapping between the numbers 0 to 99 (designated here as  $N$ ) and  $\Lambda$  is given by Table 1. The distribution of  $\Lambda$  given by Table 1 is based upon the results of Rosenberg and Dewan.<sup>1</sup> While there remain some unanswered questions regarding the accuracy of this distribution at this time, it is possible to say that it is a reasonable one to use for simulation purposes. The actual resulting value of  $K_B$  that will emerge, however, will be, for present purposes, regarded as arbitrary. In other words, the purpose of this paper is to develop a method of

describing turbulent transport in a stable fluid in general, and its application to specific data will be done elsewhere.

Table 1. Distribution of Layer Thicknesses  $\Delta$

N Range	$\Delta$
$0 \leq N \leq 53$	$3\Delta z$
$53 < N \leq 74$	$5\Delta z$
$74 < N \leq 85$	$7\Delta z$
$85 < N \leq 92$	$9\Delta z$
$92 < N \leq 99$	$11\Delta z$

In Rosenberg and Dewan<sup>1</sup> and Dewan,<sup>2</sup> some specific boundary conditions were used at the top and bottom of the slab. This caused more than one reader to raise questions, and it also gave rise to confusion about the mathematics and the physics of the situation. For this reason we devised a method that completely eliminates any boundary conditions. This is the reason that the slab in Figure 4 is located within an "environment". (The technique was suggested by Neil Grossbard, who was also responsible for writing the computer programs used below.) The random-number generator for  $z$  gave values of uniform probability from  $z = 0$  to  $z = \max$ . Layers generated outside the slab were not counted by the program, but all layers within the slab, including any points within, were counted. This count was used in a manner to be described. The point here is that the layers outside the slab served only to "cause transport" across the boundaries of the latter in a reasonable manner.

One more problem remained. The environment was finite and therefore it also had boundaries. Thus, there was the question of how to account for the effects of these boundaries. The "environment" was chosen to be much larger than the slab, and the slab itself was located in the center of the environment, as indicated. A technique to be described was used to trace the influence of the bounds of the environment. This influence propagated toward the slab, and at the moment it reached the slab (if it ever did), the program would automatically terminate.

The following procedure was used to trace the influence of the boundaries at  $z = 0$  and  $z = \max$ . As soon as a layer was generated which in any way contacted the boundary, a "cursor" (shown in Figure 4 as an arrow) would be placed (in effect) at the edge of this layer which was nearest to the slab. When a subsequent layer overlapped the cursor, the latter was moved again to that layer edge nearest

to the slab. At the bottom of Figure 4, this has occurred twice, and at the top, three times. The number generator would generate numbers exclusively for values of  $z$  which were between the upper and lower cursors and the program would terminate if either cursor came within a distance  $11\Delta z$  of the slab. Thus, the boundaries had no effect on the calculation of flux through the slab.

In order to calculate  $K_B$ , the program, in effect, measured the flux,  $\bar{F}$ , out of the bottom of the slab, and used Eq. (3), as was mentioned.  $\partial\phi/\partial z$  was taken as  $R^{-1}$ , which was justified not only from the reasonableness of the assumption of constant  $\partial\phi/\partial z$  in a steady state process, but also by the actual results to be displayed below (see Figure 8 D through I). We now consider exactly how  $\bar{F}$  is calculated.

As mentioned,  $\bar{F}$  is the amount of "material mixed out" of the bottom of the slab per unit of time. The time was calculated by adding 1 to a register labeled KOUNT each time a layer included a point interior to the slab. The total time  $t$  was calculated from

$$t = (\text{KOUNT}) \cdot \Delta t \quad (12)$$

where  $\Delta t$  is the time interval between layer formations within the slab. This quantity,  $\Delta t$ , is to be regarded as the average time between layer formations in the actual situation which involves random times for layer formations, but the exact connection between  $\Delta t$  and actual measurements will be described below. The average flux will be the total amount of material (per unit of area) to exit the bottom of the slab (at the time  $t$ ) divided by  $t$ . How is the amount of material mixed out in one mixing event across the boundary to be calculated? This perhaps explained most simply by means of a specific example. Let the thickness be  $\Lambda = 5 \Delta z$ , and let it be positioned across the lower slab boundary, as shown in Figure 5. Let the values of  $\phi$  at the center of each "cell" of the layer be given as indicated in this figure, that is by  $\phi_1$  to  $\phi_5$ . Only the two uppermost cells will be within the slab, and the rest will be below. We wish to calculate how much material per unit of area is removed from the two upper cells by the "mixing" or averaging process.

The initial amount of material,  $M_i$ , in the upper cells (remembering that  $\phi$  here will be a density) is

$$M_i = A\Delta z (\phi_4 + \phi_5) \quad (13)$$

where  $A$  is the area. After the value of  $\phi$  has been made homogeneous (within  $\Lambda$  by mixing or, equivalently, by averaging) the new amount of material in the two top cells,  $M_p$ , is

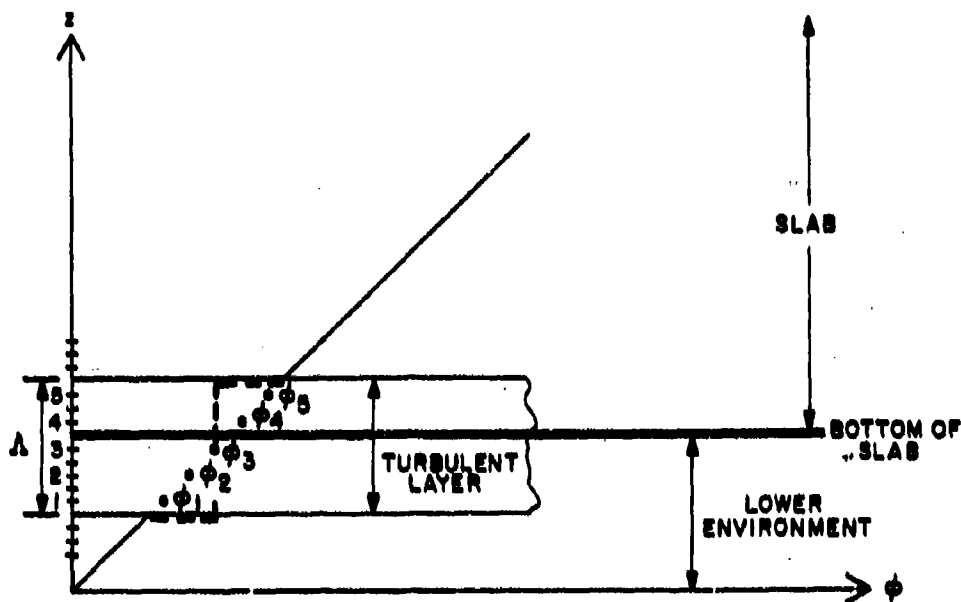


Figure 5. Explanation of the Calculation of  $K_b$  by Means of Flux Out of the Bottom of the Slab by Means of a "Mix-Through" Process

$$M_f = (A\Delta z) \left( \frac{2}{5} \right) (\phi_1 + \phi_2 + \phi_3 + \phi_4 + \phi_5) \quad (14)$$

The amount of material per unit area passing through the boundary by this mixing process is given by

$$\text{DUMP} = \frac{M_i - M_f}{A} \quad (15)$$

In general, the values of  $M_i$  and  $M_f$  would depend upon layer thickness and location, etc. Each time such an event occurred, an amount given by Eq. (15) was added to a register called DUMP. Thus, DUMP, at any time  $t$ , was the total output per unit area. The average flux,  $\bar{F}$ , was therefore calculated from

$$\bar{F} = \frac{\text{DUMP}}{\Delta t \cdot \text{COUNT}} \quad (16)$$

hence, from Eqs. (16), (3) and  $\partial\bar{\phi}/\partial z = R^{-1}$ , we obtain

$$K_{B-FLUX} = \left( \frac{DUMP \cdot R}{\Delta t \cdot COUNT} \right) \quad (17)$$

where the subindex "FLUX" will distinguish the estimate of  $K_B$  from others to be described below.

The actual simulation results from Eq. (17) will be shown in Section 8. First, however, some other methods to estimate  $K_B$  will be described. The latter are based on the idea that solutions to the diffusion equation will depend on a constant value  $K_B$ , which is to say that  $K_B$  will be independent of initial or boundary conditions. We shall consider three specific cases and determine if the estimates of  $K_B$  based upon continuous theory and simulated behavior is self-consistent. These cases are (a)  $\phi(z)$  initially is a delta function at the center of the slab, (b) the initial  $\phi(z)$  interior to the slab is a constant (with respect to  $z$ ) and the "walls" are "held" to a different constant value higher than the interior value, and (c)  $\phi(z)$  is a straight line, and the slab boundaries are insulated from the "environment". In effect,  $K_B$  will be estimated from the diffusion effects in these three cases.

### 5. CALCULATION OF $K_B$ FROM DIFFUSIVE EFFECTS

In this section, we examine the solutions to the continuous, one-dimensional, diffusion equation for the purpose mentioned above.

#### 5.1 Delta Function

The one-dimensional diffusion equation is

$$K \frac{\partial^2 \phi}{\partial x^2} = \frac{\partial \phi}{\partial t} \quad (18)$$

The solution in the case where the initial  $\phi$  distribution is a delta function is well known (see Carrier and Pearson, pp. 28-34<sup>10</sup>). It is given by

$$\phi(t, z) = \frac{1}{2\sqrt{Kt}} e^{-(z-z_0)^2/(4Kt)} \quad (19)$$

10. Carrier, G.F. and Pearson, C.E. (1976) Partial Differential Equations, Academic Press, Inc.

where  $z_0$  designates the initial location of the delta function. The domain of this solution is  $-\infty < z < \infty$ , and there are no boundary conditions. (Equation (19) is the Green's function when the initial condition on  $\phi(z)$  is specified.)

Given the behavior of  $\phi(z, t)$  under these conditions, one can estimate  $K$  from the rate of spread in a simple way, that is by measuring the  $1/e$  halfwidth,  $r_e$ , at a given time. The latter is obtained from Eq. (19) by setting the exponent equal to -1. Solving for  $K$

$$K_{B-DELTA} = \left( \frac{r_e^2}{4t} \right) \quad (20)$$

(Note that the "decay," as used here, is spatial, not temporal.) Thus,  $K$  can be estimated by the amount of spread of the initial delta function. A refined estimate could be obtained by appropriately combining several such measurements (taken at a number of times). This, however, was not done here. Figure 8 shows schematically the typical behavior to be expected, that is, the function decreases in height and it spreads as time increases.

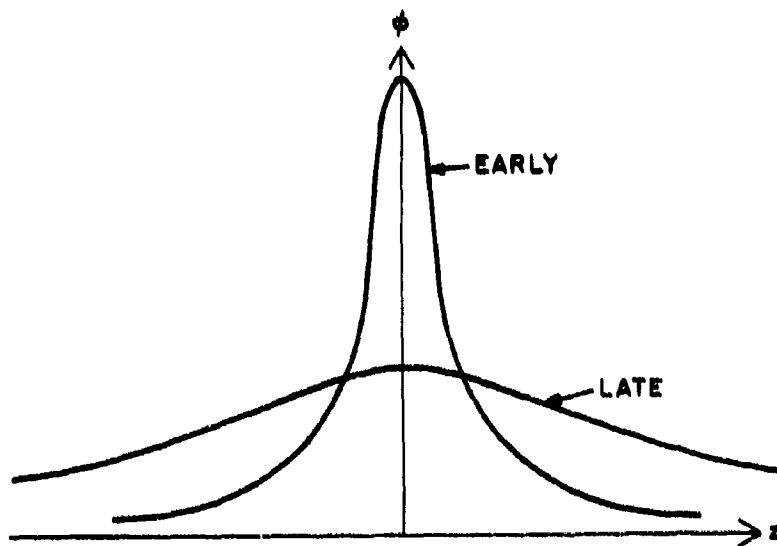


Figure 8. Schematic Drawing of Delta Function Diffusion Expected from Continuous Theory

### 5.2 Intrusion from Boundaries

Next we consider the case where we have a slab such that  $\phi(z, 0) = 0$  inside and  $\phi(z, 0) = \phi_0$  (a constant larger than zero) outside. We assume infinite conductivity outside, and we want to know  $\phi(z, t)$  inside (that is, the development of  $\phi$  inside as a function of time). Notice that, as was the case for Figure 6, the slab is turned sideways, with  $z$  going to the right in Figure 7. Figure 7(a) shows the initial condition while Figure 7(b) shows schematically how  $\phi$  diffuses inwards from the boundary. The exact solution of Eq. (18) for the semi-infinite slab case will be found in Spiegel, p. 222.<sup>11</sup> (For early times, in our form of simulation, the intrusions from the two sides will not influence each other at all, and therefore this solution will suffice for our needs.) This solution is:

$$\phi(z, t) = \phi_0(1 - \text{erf}(y)) \quad (21)$$

which in Figure 7 would apply only to the left side. The definitions of  $y$  and  $\text{erf}(y)$  are

$$y = \frac{z}{(2\sqrt{Kt})} \quad (22)$$

and

$$\text{erf}(y) = \frac{2}{\sqrt{\pi}} \int_0^y e^{-u^2} du \quad (23)$$

A tabulation of the values of  $\text{erf}(y)$  is to be found in Abramowitz and Stegun, p. 911.<sup>12</sup> With this formulation, one can start with a given  $\phi(z, t)$  (from the simulation) and estimate  $K$  numerically in the following manner. First,  $y$  is estimated via Eq. (21), from a given  $\phi(z, t)$  for a particular choice of both  $z$  and  $t$ . Then solving Eq. (22) for  $K$

$$K_{B-INT} = \left(\frac{1}{t}\right) \left(\frac{z}{2y}\right)^2 \quad (24)$$

11. Spiegel, M.R. (1968) Theory and Problems of Laplace Transforms, Schaum Publishing Co.

12. Abramowitz, M. and Stegun, I.A. (1964) Handbook of Mathematical Functions, N.B.S. Appl. Math. Series #55.



and since  $z$ ,  $t$ , and (from the tables)  $y$  are all known,  $K$  can be estimated. The subscript "INT" stands for intrusion,

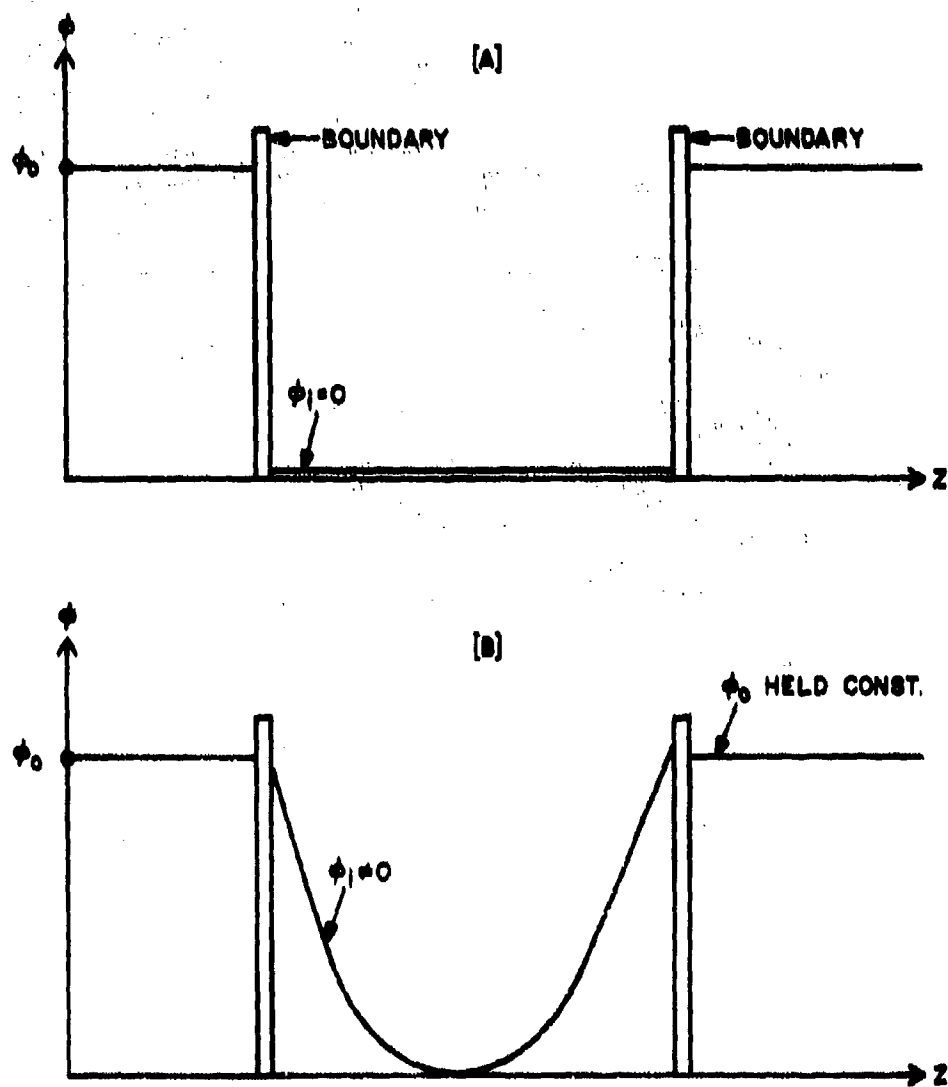


Figure 7. Expected Behavior of Diffusion Through Boundaries in Continuous Theory of Diffusion

### 5.3 Insulated Slab—Initially Linear $\phi(z,0)$

Figure 8 depicts a slab with initial distribution of  $\phi$  given by

$$\phi = az \quad (25)$$

where

$$a = \frac{\phi_0}{R} \quad (26)$$

and the thickness of the slab is given by  $R$  and maximum  $\phi$  by  $\phi_0$ . We assume that the slab is insulated at the boundaries, therefore

$$\left. \frac{\partial \phi}{\partial z} \right|_{z=0, z=R} = 0 \quad (27)$$

These boundary conditions are explained in any book on heat conduction. The analytic solution of Eq. (18) with these conditions is (see for example, Dewan<sup>3</sup>)

$$\phi(z,t) = \phi_0 \left\{ \frac{1}{2} + \frac{4}{\pi^2} \sum_{n=1}^{\infty} \frac{g(n)}{n^2} \cos \left( \frac{n\pi z}{R} \right) e^{-K(\pi/R)^2 t} \right\} \quad (28)$$

where  $g(n)$  is defined by

$$g(n) = \begin{cases} 0 & n \text{ even} \\ -1 & n \text{ odd} \end{cases} \quad (29)$$

Define the symbol  $A_1(t)$  to be the amplitude of the first harmonic of the solution of Eq. (28). Thus

$$A_1(t) = (-0.405) e^{-K(\pi/R)^2 t} \quad (30)$$

This is obtained from Eq. (28) by setting  $z = 0$ , calculating  $4/\pi^2 = 0.405$ , regarding the factor  $(1/2)$  as the zeroth harmonic and setting  $\phi_0 = 1$  for convenience from this point on.

Suppose that we are given  $\phi(z,t)$  (from the numerical simulation), and we wish to calculate  $K$  from this solution. The procedure we shall use is to calculate the first harmonic numerically, and to thus ascertain  $A$  at a given value of  $t$ . Then  $K$  can be estimated by solving Eq. (30) for  $K$ :

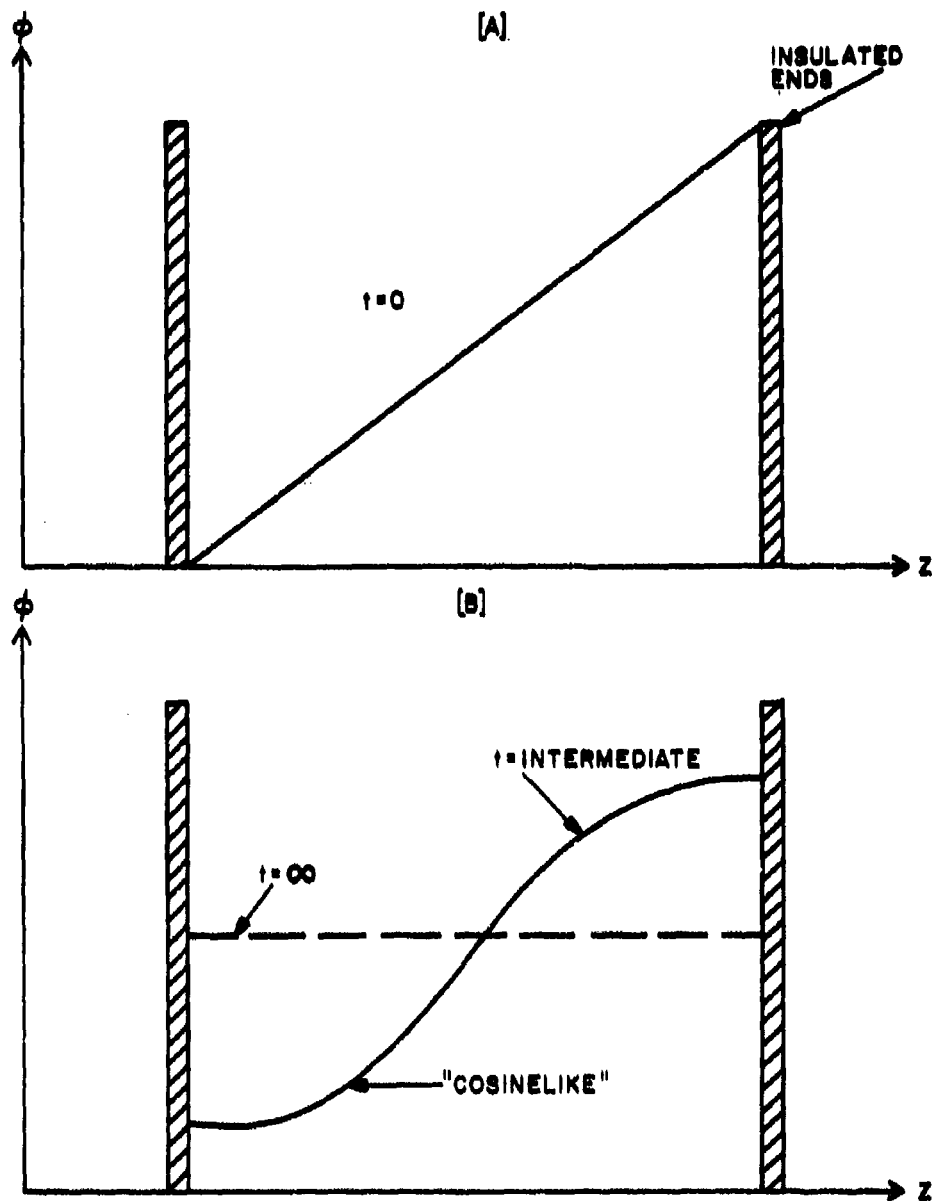


Figure 8. Expected Behavior of Temperature Inside an Insulated Slab with Initially Linear Temperature Profile. As time passes, the higher harmonics quickly damp and only the first harmonic would survive visibly

$$K_{B-INSUL} = \left[ -\ln \left( \frac{A_1(t)}{-0.408} \right) \right] \left( \frac{R}{\pi} \right)^2 \left( \frac{1}{t} \right) \quad (31)$$

We now have the means to estimate the bulk diffusion parameter,  $K_B$ , directly from solution behavior for the three special cases of interest. We now turn to the actual simulations of the random mixing layer situation.

## 6. CONNECTIONS OF CERTAIN PARAMETER VALUES TO EXPERIMENTAL DATA AND SIMULATIONS OF MIXING LAYER TRANSPORT

### 6.1 Relations Between Parameters $\Delta t$ and $\Lambda$ and Possible Measurements

Simulations in general can be performed only for numerically specific cases. In this subsection, we wish to justify that a certain choice for  $\Delta t$  and  $\Lambda$  is a reasonable one in connection with atmospheric studies. We also wish to show how these parameters could be measured in practice.

How could one measure  $\Lambda$ , the turbulent layer thickness? One method that has been employed (Barat<sup>13</sup>) uses a high-resolution wind fluctuation measuring device mounted on a balloon. When the balloon descends through a turbulent layer, the turbulent fluctuations can be detected, and the information telemetered to a ground station. Such measurements made in the stratosphere indicate that a typical value of  $\Lambda$  would be around 200 m.

An alternative measurement technique estimates  $\Lambda$  from the Richardson number profiles (Rosenberg and Dewan<sup>1</sup>). The present model was originally created for exactly this purpose. (In other words, we needed a method to convert  $R_i$  profiles into estimates of transport.) The Richardson number profiles are ascertained from measurements of the horizontal winds as a function of altitude, in conjunction with the vertical profile of the temperature as well. Triangulated rocket-laid smoke trails is the method of choice for high-resolution wind profiles. The estimates of  $\Lambda$  can be obtained from the fact that when the Richardson number,  $R_i$ , is less than 0.25, the layer will, presumably, become turbulent. When account is taken of subsequent spreading of the layer,  $\Lambda$  can be estimated. According to Rosenberg and Dewan, <sup>1</sup>  $\bar{\Lambda} \sim 200$  m is a reasonable number as estimated by this technique. For further discussion, see Dewan.<sup>2</sup>

The parameter  $\Delta t$  (which stands for "time between onsets of layer formation" in the simulations to be given below) is measured less directly, and is tied methodologically to the method of estimating  $\Lambda$ . In the case where  $\Lambda$  is measured

13. Barat, J. (1975) Etude Experimentale de la Structure du Champ de Turbulence dans la Moyenne Stratosphere, C.R. Acad. Sc. Paris, 280, Ser. B, pp. 691-693.

from  $R_i$  profiles, the following method is appropriate. First (see Rosenberg and Dewan,<sup>1</sup> and Dewan,<sup>2</sup>) we make the simplifying assumption that, if over a certain height region (slab) there are usually several layers detected, then such a profile will, on the average, be replaced by another profile at a time  $\Delta t_f$  later. The sub-index,  $f$ , is for "time frame". The simplification consists of replacing the random times of layer formation by  $\Delta t_f$  between profiles. Once  $R_i < 0.25$ , the layer to be considered is unstable; however, a certain time must elapse before the instability is replaced by an actual "breakdown" and subsequent turbulence. Shortly after the latter occurs,  $R_i$  will rise again above the threshold value (to a value of 0.7, perhaps), and the turbulence will begin to decay. At this point, the  $R_i$  profile would no longer indicate the subsequent generation of the turbulent layer. Based upon the measurements of Browning<sup>14</sup> of Kelvin-Helmholtz billows in the atmosphere by means of radar and balloon measurements, it was estimated (Rosenberg and Dewan<sup>1</sup>) that  $\Delta t_f \sim 1800$  s.<sup>†</sup> In order to ascertain  $\Delta t$  from  $\Delta t_f$ , one must first estimate the average number of layers to be found at any time in the slab, designated below as  $n$ . Then

$$\Delta t = \frac{\Delta t_f}{n} \quad (32)$$

If, for example,  $P^*$  designates the average fraction of the slab of thickness  $R$  that is turbulent, and suppose we are given  $\bar{\Lambda}$ , the average turbulent layer thickness, then

$$n = \frac{P^* R}{\bar{\Lambda}} \quad (33)$$

from  $P^* = (n\bar{\Lambda} / R)$ .

In the case where the profile of turbulence is estimated by means of in-situ measurements of velocity fluctuations,  $\Delta t_f$  would correspond to the average time for the average layer to decay (from time of measurement) to the level where it would be below the "threshold intensity" and would be called laminar. Based upon this given threshold,<sup>‡</sup>  $P^*$  would be ascertained (as well as  $\bar{\Lambda}$ ), and again  $\Delta t$  would be estimated from Eqs. (32) and (33). For further discussion, see Dewan.<sup>2§</sup>

<sup>†</sup> Actually,  $\Delta t_f$  would correspond to the average time between the observation of  $R_i < 0.25$  and breakdown. The latter would depend on growth at time of observation and  $R_i$ .

<sup>‡</sup> If the threshold were high,  $P^*$  would be measured as small, but so also would  $\Delta t_f$  (because the layers would disappear more rapidly below threshold). We assume here that the ratio  $(P^* / \Delta t_f)$  remains independent of the threshold over a reasonable range of the latter.

<sup>§</sup> In this simulation  $\sqrt{\bar{\Lambda}^2} = 277$  m, whereas  $\bar{\Lambda} = 240$  m.

14. Browning, K.A. (1967) Structure of the atmosphere in the vicinity of large amplitude Kelvin-Helmholtz billows, Roy. Met. Soc. Quart. J. 97:283-299.

## 6.2 Simulation Results

### 6.2.1 $K_{B-FLUX}$

Figure 9 (A-C) shows the value of  $K_{B-FLUX}$ , based on Eq. (17), as a function of time. As the time base (number of "counts" or layer mixing events) increases,  $K_{B-FLUX}$  converges to a fixed value. Parameters were assigned as follows.  $R = 400$  points, and  $\Delta z = 50$  m; where  $R = 20 \times 10^3$  m. Also,  $\bar{\lambda} = 240$  m and  $\sqrt{\bar{\lambda}^2} = 277$ , as determined from the distribution designed into Table 1. From Rosenberg and Dewan's<sup>1</sup> result of  $\Delta t_f = 1500$ s, we use

$$\Delta t = \left(\frac{\bar{\lambda}}{R}\right) \left(\frac{\Delta t_f}{P^*}\right) = \left(\frac{240}{20 \times 10^3}\right) \left(\frac{1500}{0.05}\right) = 360s \quad (34)$$

where  $P^* = 0.05$  is taken from the same reference. The simulation  $K_{B-FLUX} = 0.311 \text{ m}^2/\text{s}$ .

Figure 9 (D-I) shows the important result that  $\phi(z)$  is essentially unchanged during this simulation.

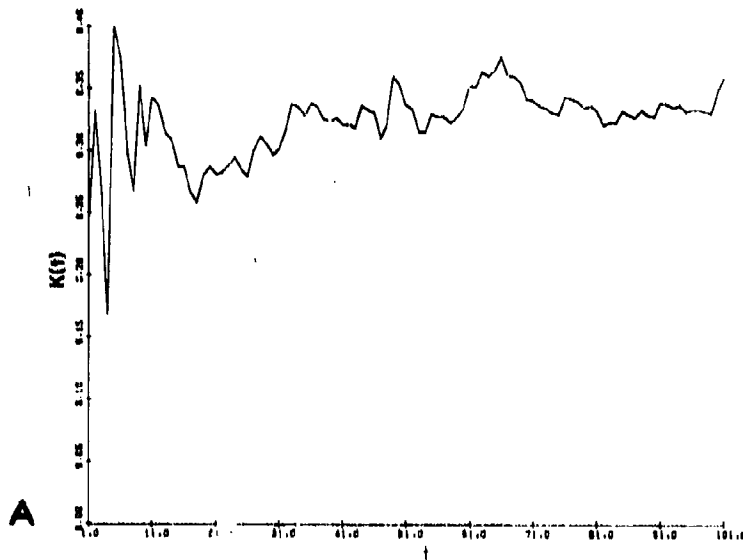


Figure 9. Bulk Diffusivity,  $K_B$  (as Calculated in the Simulation Via the Flux) as a Function of Time. (a-c) Time is given in terms "mix through" events. 100 ~ 8,000 mixing event. Parts d through i show the initial and subsequent profiles in order to demonstrate that the mean slope of  $\phi$  remains essentially constant. (The profiles are shown at intervals of 5,000 mixing events)

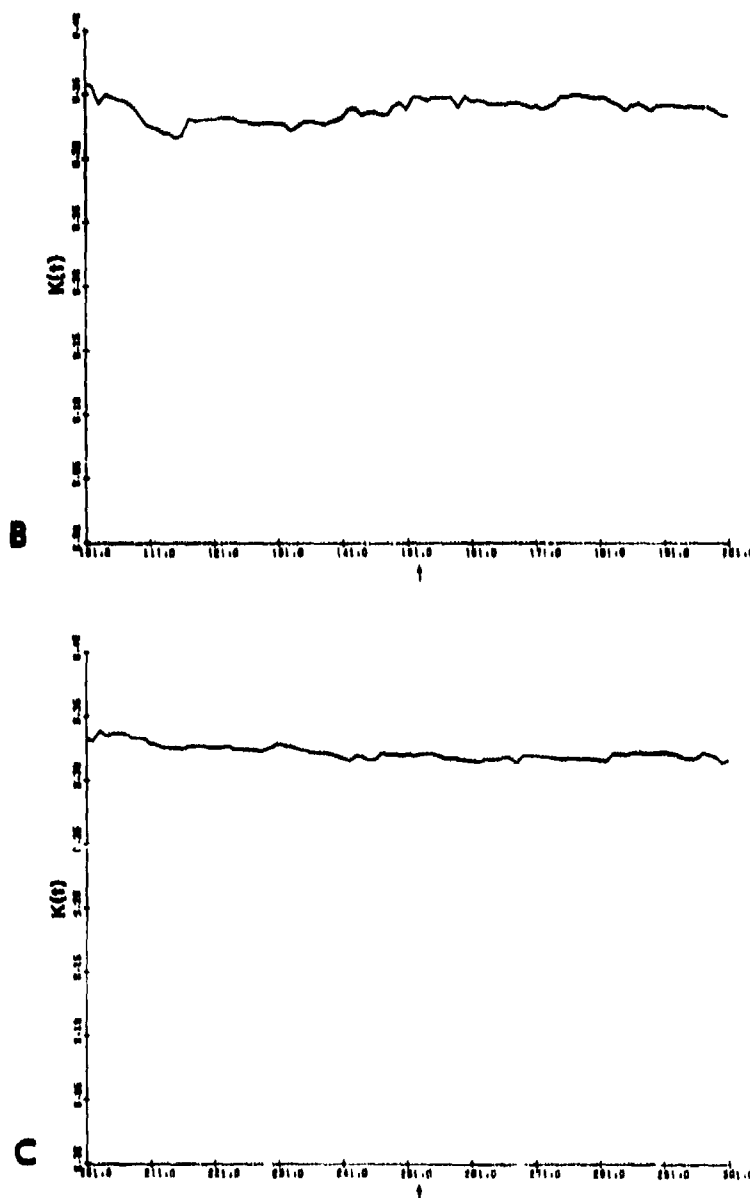


Figure 9. Bulk Diffusivity,  $K_B$  (as Calculated in the Simulation Via the Flux) as a Function of Time. (a-c) Time is given in terms "mix through" events. 100 ~ 8,000 mixing event. Parts d through i show the initial and subsequent profiles in order to demonstrate that the mean slope of  $\phi$  remains essentially constant. (The profiles are shown at intervals of 5,000 mixing events)

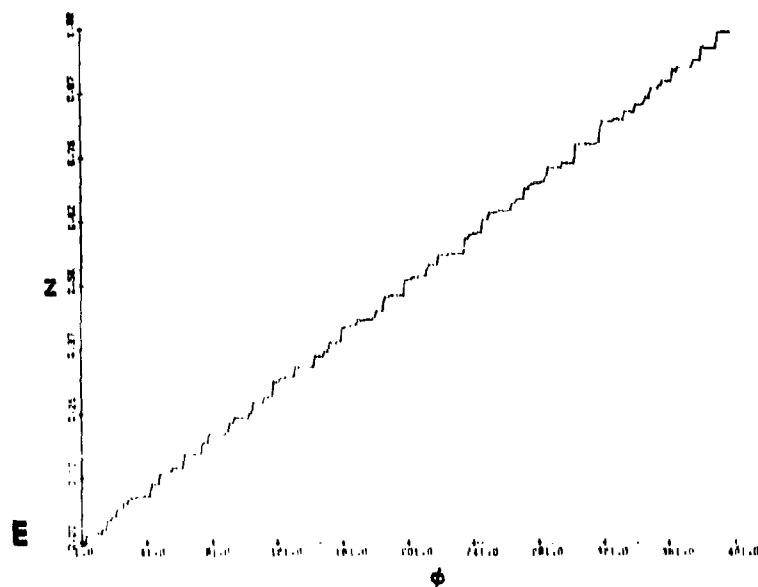
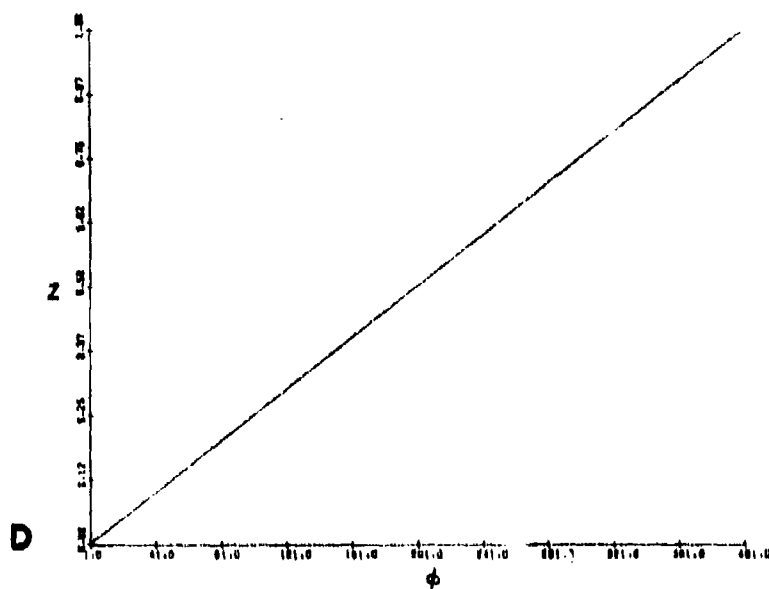


Figure 8. Bulk Diffusivity,  $K$  (as Calculated in the Simulation Via the Flux) as a Function of Time. (a-e) Time is given in terms "mix through" events. 100 ~ 8,000 mixing event. Parts d through i show the initial and subsequent profiles in order to demonstrate that the mean slope of  $\phi$  remains essentially constant. (The profiles are shown at intervals of 5,000 mixing events)



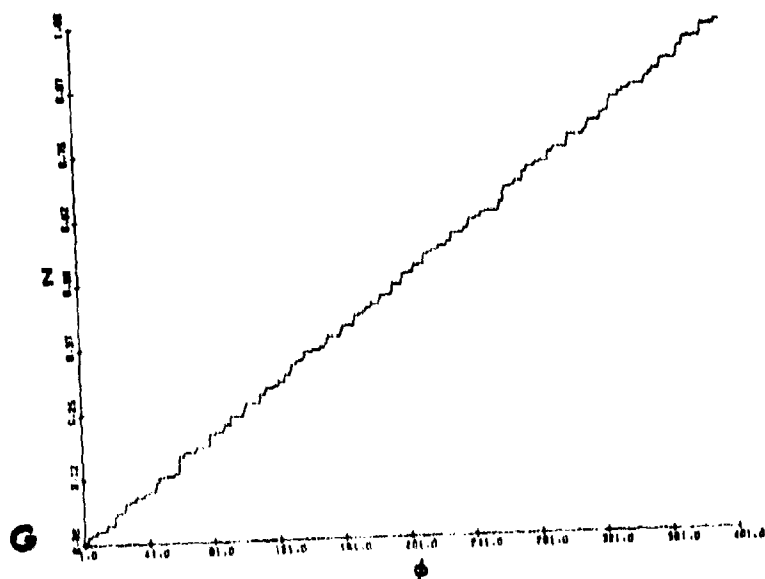
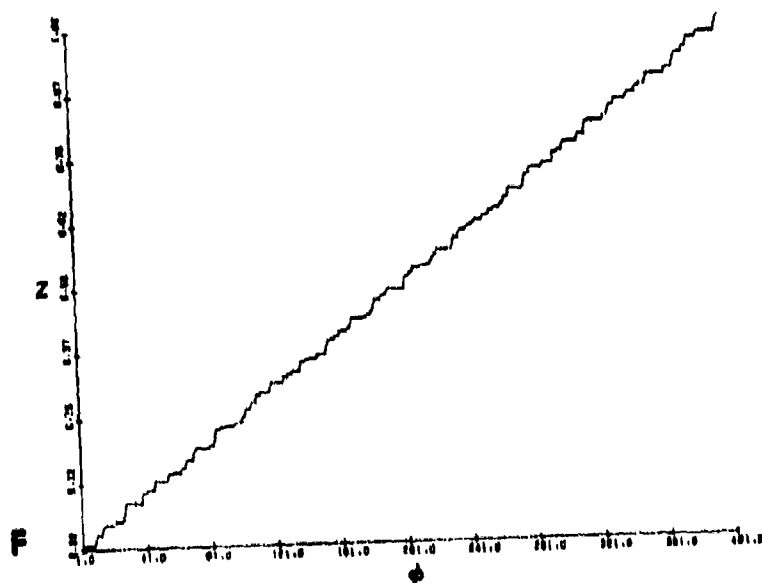


Figure 9. Bulk Diffusivity,  $K$  (as Calculated in the Simulation Via the Flux) as a Function of Time. (a-c) Time is given in terms "mix through" events. 100 ~ 8,000 mixing event. Parts d through f show the initial and subsequent profiles in order to demonstrate that the mean slope of  $\phi$  remains essentially constant. (The profiles are shown at intervals of 5,000 mixing events)

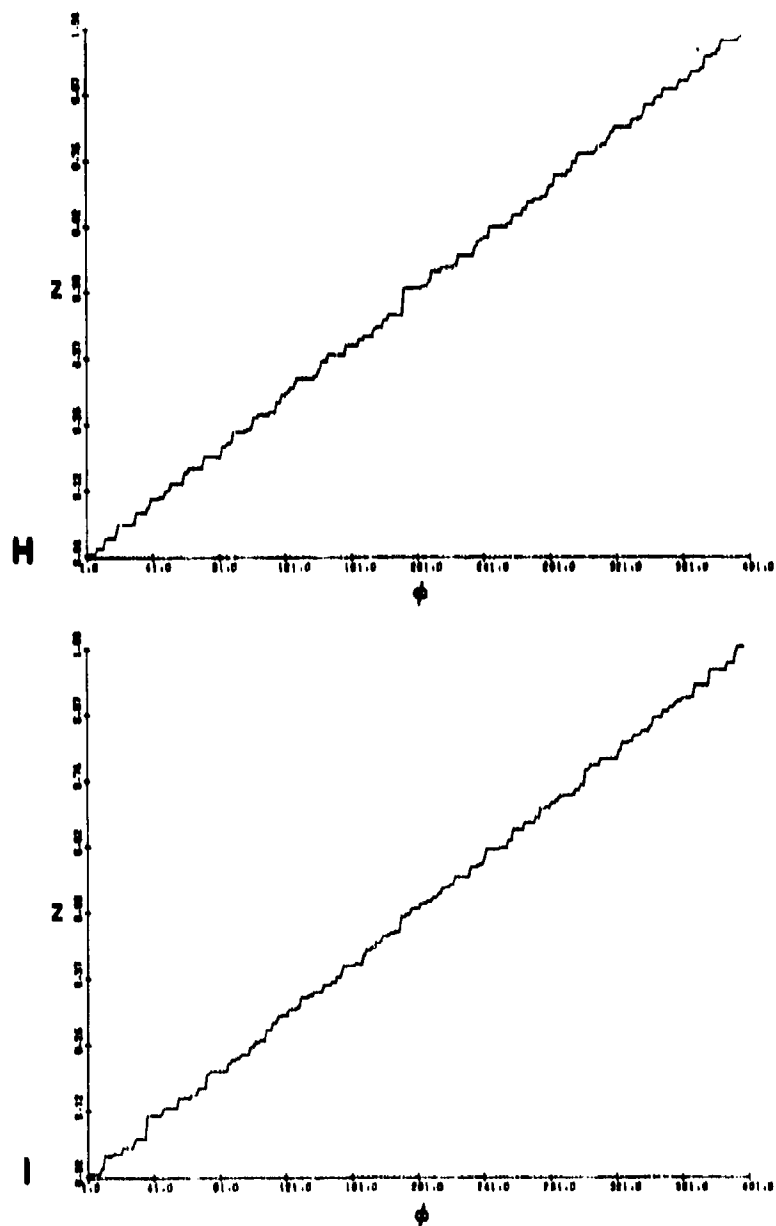


Figure 9. Bulk Diffusivity,  $K_B$  (as Calculated in the Simulation Via the Flux) as a Function of Time. (a-c) Time is given in terms "mix through" events, 100 ~ 8,000 mixing event. Parts d through f show the initial and subsequent profiles in order to demonstrate that the mean slope of  $\phi$  remains essentially constant. (The profiles are shown at intervals of 8,000 mixing events)

### 6.2.2 $K_{B-DELTA}$

Figure 10 (A through H) (compare the continuous case) shows the results a sequence of layer mixing events upon an initial  $\phi(z, 0)$ , which is a delta function. In this numerical simulation it is given by zero for all points in the range, R (of 400 points), except for the center point ( $z_0$ ), which was set to the maximum value (100). At the arbitrary  $t$   $KOUNT = 30.4 \times 10^3$  (30,400 layer formations), and with 360 seconds assigned to each count,  $K_{B-DELTA}$  was estimated from Eq. (20). The value of the peak was 3.0, having started from 100, and its  $(1/e)$  value is therefore 1.1. The values of the end points of the two  $r_e$  (one per side) were estimated from the printout. They occurred at  $z =$  point 125 and point 275. The center was located at point 200. Thus, using  $\Delta z = 50$  m, the average  $r_e$  was determined to be  $r_e = (3700)$  meters, thus

$$K_{B-DELTA} = \frac{(3700)^2}{(4)(360)(30,400)} = 0.31 \text{ m}^2/\text{s} \quad (35)$$

which agrees with  $K_{B-FLUX}$ .

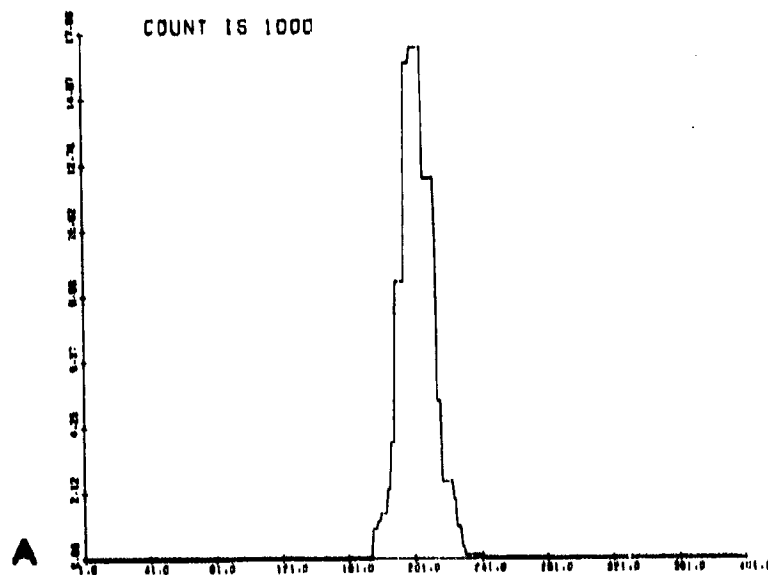


Figure 10. Simulated Evolution of Delta Function When Exposed to Random Mixing Layers. A 3-D plot, H, summarizes the evolution

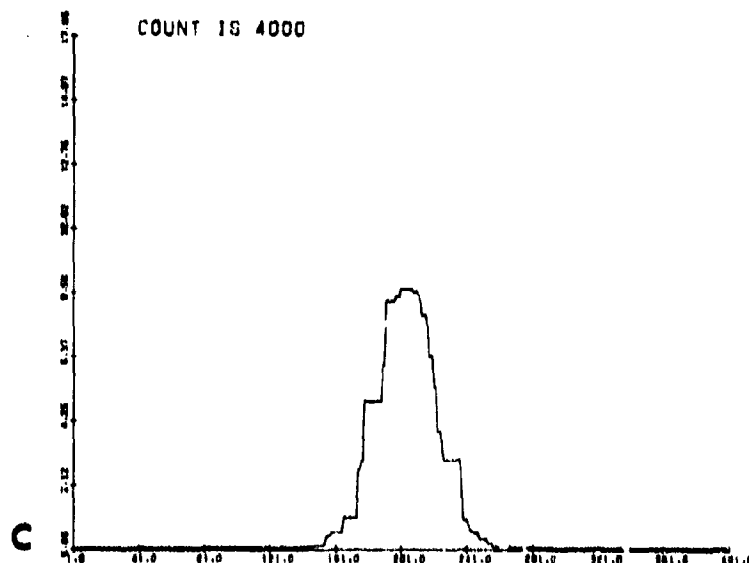
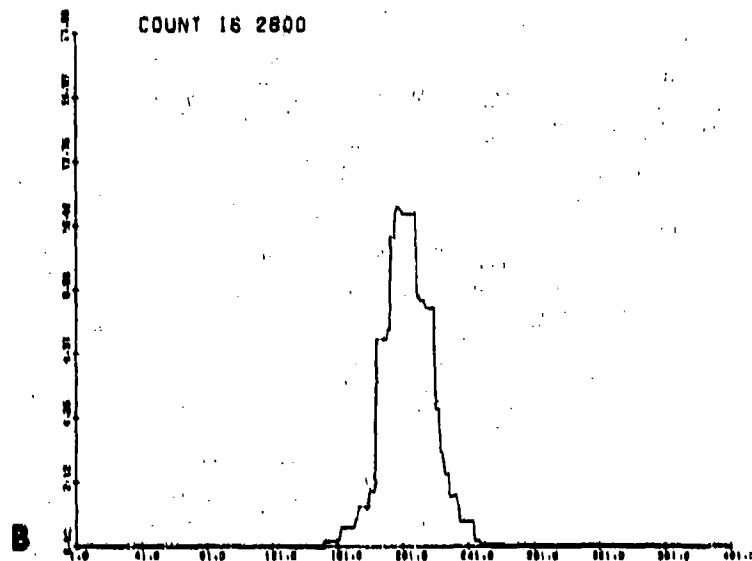


Figure 10. Simulated Evolution of Delta Function When Exposed to Random Mixing Layers. A 3-D plot, H, summarizes the evolution

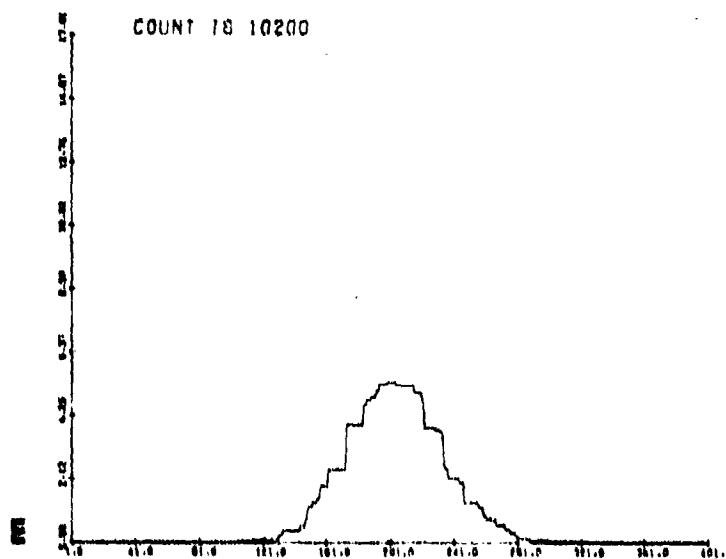
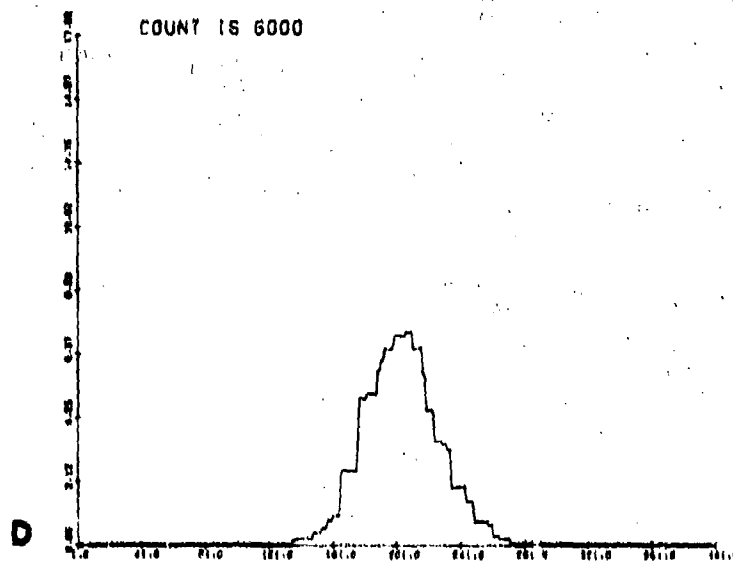


Figure 10. Simulated Evolution of Delta Function When Exposed to Random Mixing Layers. A 3-D plot, H, summarizes the evolution

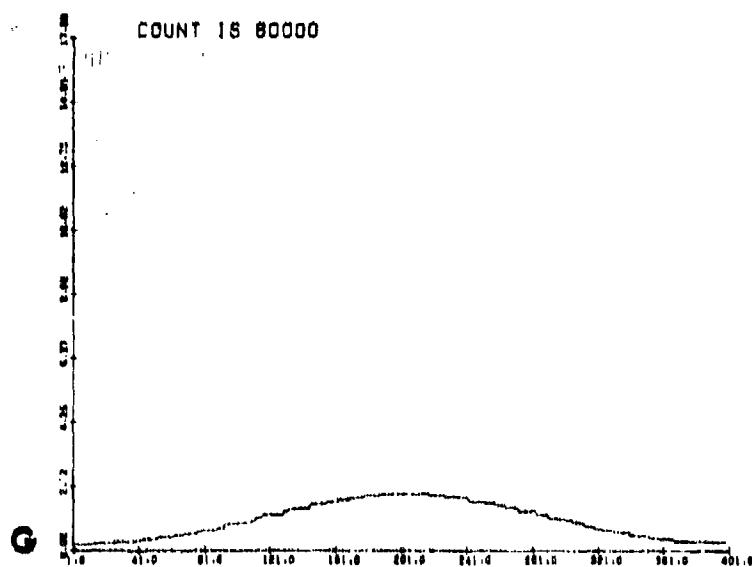
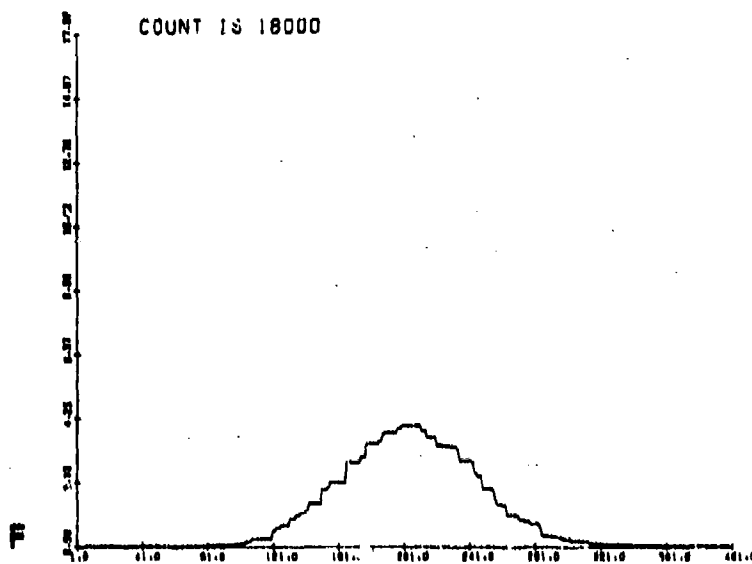


Figure 10. Simulated Evolution of Delta Function When Exposed to Random Mixing Layers. A 3-D plot, H, summarizes the evolution

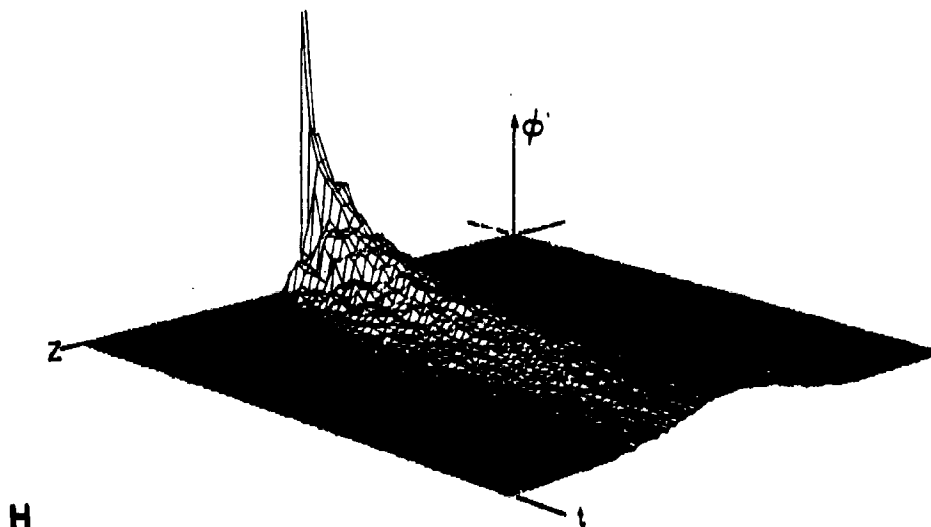


Figure 10. Simulated Evolution of Delta Function When Exposed to Random Mixing Layers. A 3-D plot, H, summarizes the evolution

### 6.2.3 $K_B$ -INTR

Figure 11 (A through D) shows the sequence for the intrusion case. At  $KOUNT = 14 \times 10^3$ , the value of  $z$  was arbitrarily chosen to correspond to point number 51, or  $51 \times (50 \text{ m/pt.}) = 2.55 \times 10^3 \text{ m}$ , from the origin. From the printout,  $\phi = 0.167$  at that point and time. The value of  $t$  was determined from

$$t = KOUNT (360) \quad (36)$$

or  $t = 5.04 \times 10^6 \text{ s}$ . From Eq. (21) ( $\phi_0 = 1$ )

$$\text{erf}(y) = 1 - 0.167 = 0.833 \quad (37)$$

Using the tables in Abramowitz and Stegun,<sup>12</sup> we found  $y = 0.98$ . Thus, from Eq. (24)

$$K_{B-INT} = \frac{1}{5.04 \times 10^6} \left( \frac{2.55 \times 10^3}{(2)(0.98)} \right)^2 = 0.34 \text{ m}^2/\text{s} \quad (38)$$

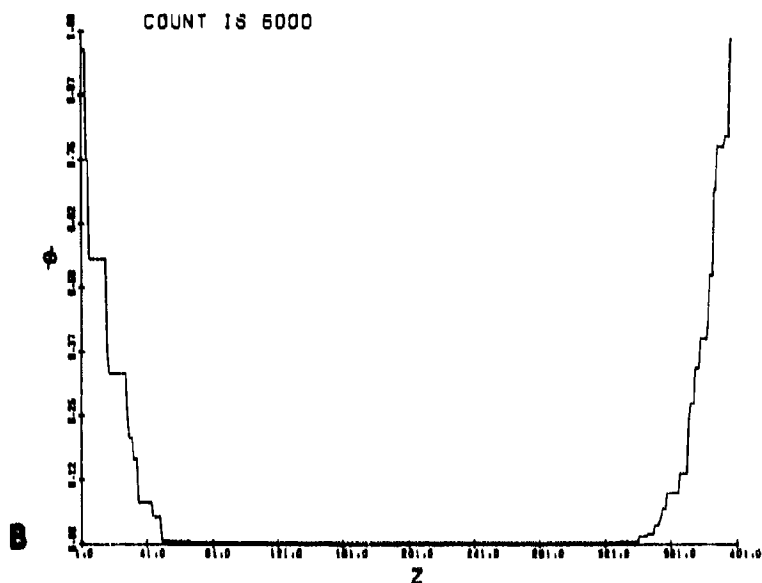
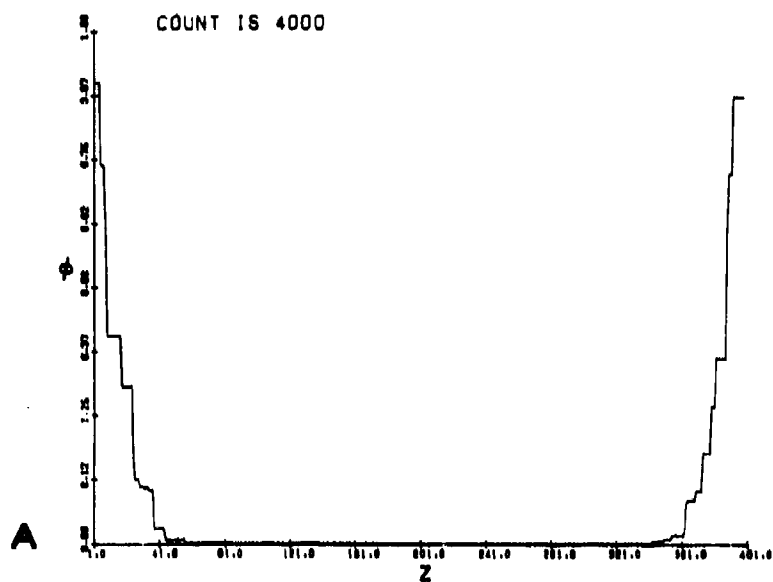


Figure 11. Simulated Evolution of the Case of Infinitely Conducting Walls and Diffusion Inwards by Means of Random Mixing Layers. 11-E is a summary 3-D plot



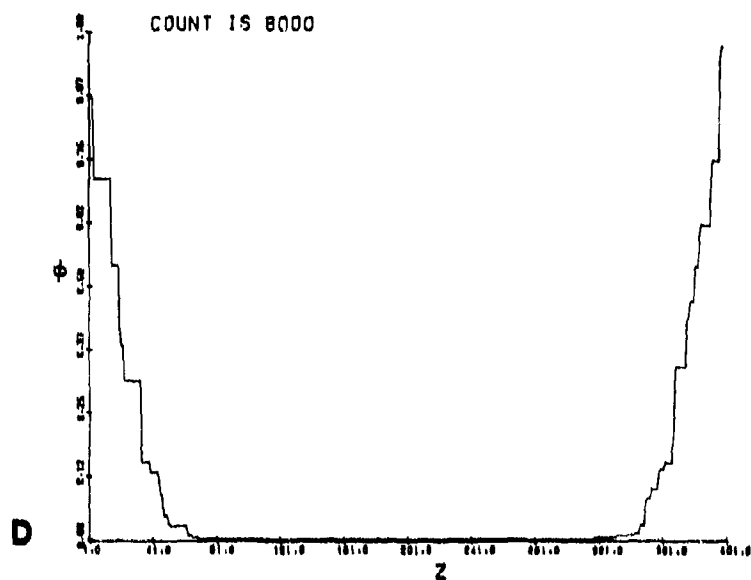
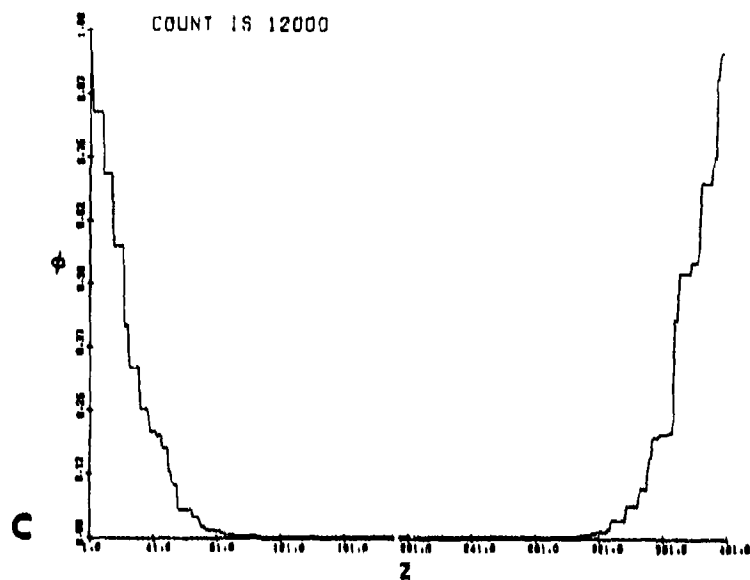


Figure 11. Simulated Evolution of the Case of Infinitely Conducting Walls and Diffusion Inwards by Means of Random Mixing Layers. 11-E is a summary 3-D plot

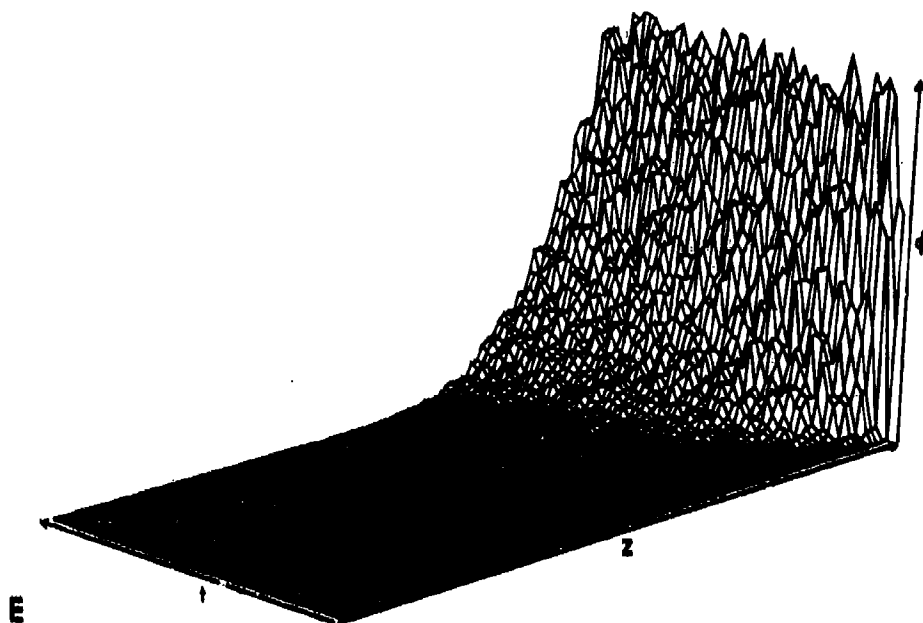


Figure 11. Simulated Evolution of the Case of Infinitely Conducting Walls and Diffusion Inwards by Means of Random Mixing Layers. 11-E is a summary 3-D plot

#### 6.2.4 $K_{B-INSUL}$

Figure 12 (A through G) shows the simulation for the case of the insulated slab. At  $KOUNT = 4 \times 10^4$  ( $t = 1.44 \times 10^7$  s), a Fourier transform was obtained from the simulated solution by means of a Fast Fourier transform analysis. This gave  $A_1(t) = (-0.381)$ . Inserting this into Eq. (31)

$$K_{B-INSUL} = \left[ -\ln \left( \frac{-0.381}{-0.408} \right) \right] \left( \frac{2 \times 10^4 \text{ m}}{\pi} \right)^2 \left( \frac{1}{1.44 \times 10^7} \right)$$

$$= 0.324 \text{ m}^2/\text{s} \quad (39)$$

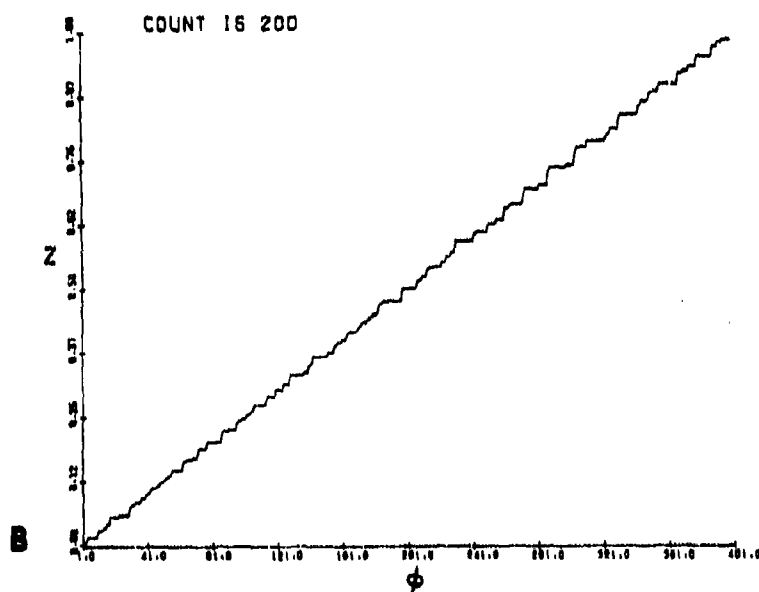
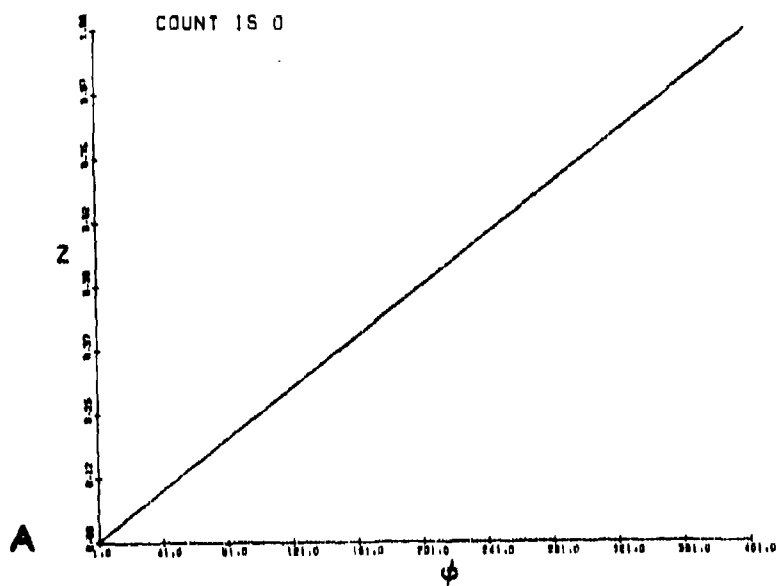


Figure 12. Simulated Evolution of "Insulated Slab" Case Via Random Mixing Layers

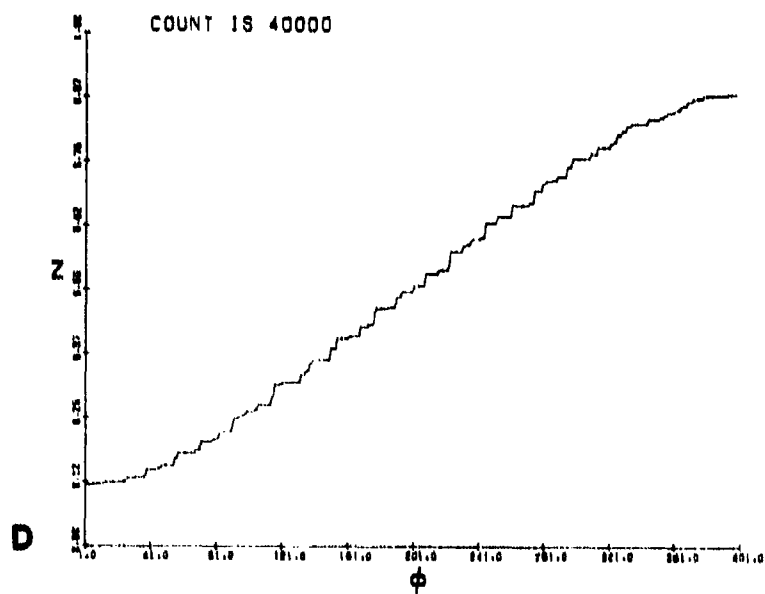
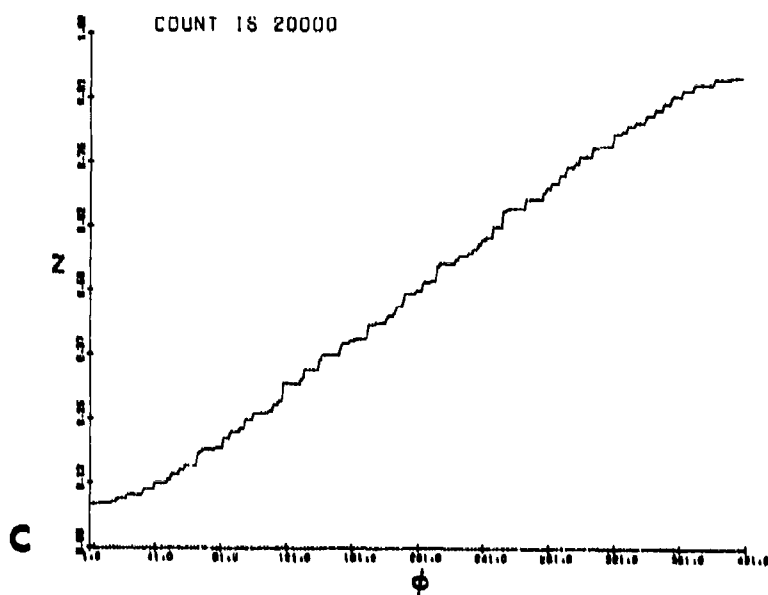


Figure 12. Simulated Evolution of "Insulated Slab" Case Via Random Mixing Layers

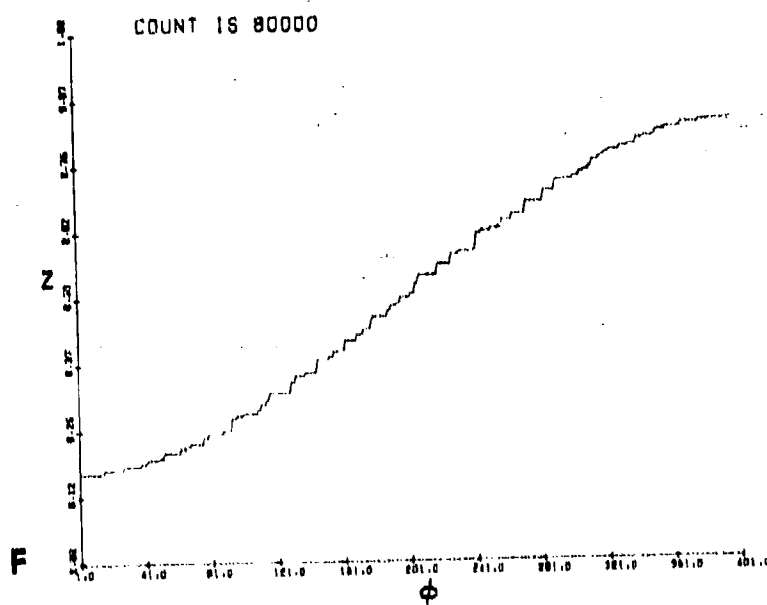
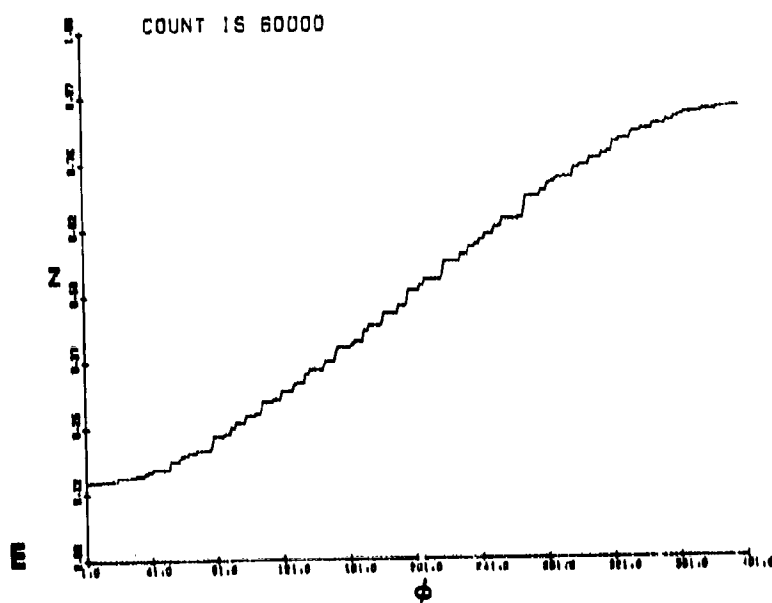


Figure 12. Simulated Evolution of "Insulated Slab" Case Via Random Mixing Layers

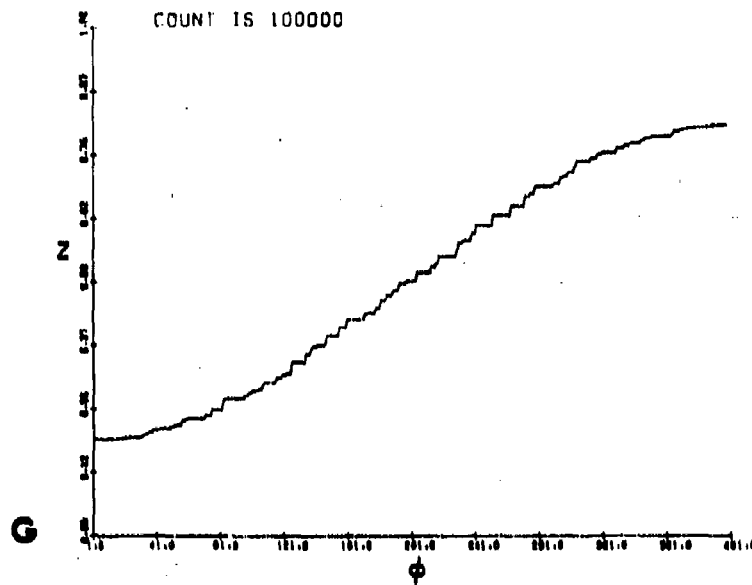


Figure 12. Simulated Evolution of "Insulated Slab" Case Via Random Mixing Layers

### 6.2.8 $K_B$ -CALC

We now use Eq. (4). Here we use

$$\Delta t_b = \frac{\Delta t_f}{P^*} \quad (40)$$

(Dewan<sup>2</sup>). Using  $P^* = 0.05$ ,  $\Delta t_f = 1500$ ,  $\sqrt{\Lambda^2} = 277$  m

$$K_{B-CALC} = \frac{(0.05)(277)^2/4}{(2)(1500)} = 0.32 \text{ m}^2/\text{s} \quad (41)$$

### 6.3 Summary of Simulation Results

Table 2 summarizes the above results, and it shows in a convincing manner that  $K_B$ , no matter which way it is estimated, gives a self-consistent result.

Table 2. Distribution Parameter,  $K_B$ , for Various Cases

$K_{B-FLUX}$	$= 0.31 \text{ m}^2/\text{s}$	$= (6.04 \times 10^{-3}) \frac{\Lambda^2}{\Delta t_f}$	$= 1.45 \times 10^{-3} (\frac{\Lambda^2}{\Delta t})$
$K_{B-DELTA}$	$= 0.31$	$= (6.04 \times 10^{-3}) \frac{\Lambda^2}{\Delta t_f}$	$= 1.45 \times 10^{-3} (\frac{\Lambda^2}{\Delta t})$
$K_{B-INTR}$	$= 0.34$	$= (6.63 \times 10^{-3}) \frac{\Lambda^2}{\Delta t_f}$	$= 1.59 \times 10^{-3} (\frac{\Lambda^2}{\Delta t})$
$K_{B-INSUL}$	$= 0.32$	$= (6.25 \times 10^{-3}) \frac{\Lambda^2}{\Delta t_f}$	$= 1.50 \times 10^{-3} (\frac{\Lambda^2}{\Delta t})$
$K_{B-CALC}$	$= 0.32$	$= (6.25 \times 10^{-3}) \frac{\Lambda^2}{\Delta t_f}$	$= 1.50 \times 10^{-3} (\frac{\Lambda^2}{\Delta t})$

The last column is rendered in units of  $\Lambda$  and  $\Delta t_f$ . This "nondimensional" form allows one to apply the formalism to fluids with other scales (for example, the ocean). Notice that only single values of  $x$  and  $t$  were used to "measure" the spread in each case,  $t$  being chosen arbitrarily. Obviously, more pairs could have been used to increase the accuracy of  $K_B$  estimates from the diffusion effects. The consistency shown in Table 2 is therefore rather remarkable, and we think one need go no farther at this point to justify the assertion that the "mixing layer"  $K_B$  of this paper is self-consistent, at least to the first significant digit.

## 7. SUMMARY AND CONCLUSIONS

In this paper, a new diffusion parameter or "effective diffusivity" has been proposed, which is designed for the extremely inhomogeneous case of layered turbulence in stratified fluids. Random occurrence in altitude, time, and layer thickness were assumed, as well as total mixing within layers. The last assumption can be relaxed, if necessary, as shown in Dewan.<sup>2</sup>

The present diffusion parameter describes a process which, in essence, is a sort of stochastic, finite difference simulation of the diffusion equation that is presumed to occur in the stratified fluids to be found in nature. While the basic assumptions remain to be verified, it is hoped that the formalism developed here will be useful in the estimation of vertical transport by turbulence in the stratosphere and upper ocean.

\*This assumes that  $P^*$  has a specific value, namely  $P^* = 0.05$ .

## References

1. Rosenberg, N.W. and Dewan, E.M. (1976) Stratospheric Turbulence and Vertical Effective Diffusion Coefficient, AFCRL-TR-75-0519, AD A019 701.
2. Dewan, E.M. (1979(a)) Estimates of Vertical Eddy Diffusion Due to Turbulent Layers in the Stratosphere, AFGL-TR-79-0042, AD A089 780.
3. Dewan, E.M. (1979(b)) Mixing in Billow Turbulence and Stratospheric Eddy Diffusion, AFGL-TR-79-0081, AD A074 486.
4. Pasquill, F. (1974) Atmospheric Diffusion, 2nd Ed., John Wiley & Sons.
5. Lilly, D.K., Waco, D.E., and Adelfang, S.I. (1975) Stratospheric mixing estimated from high altitude turbulence measurements by using energy budget techniques, The Natural Stratosphere of 1974, CIAP Monograph 1, Final Report, DOT-TST-74-51, pp. 8-81 to 8-90.
6. Panofsky, H.A. and Heck, W. (1975) Stratospheric mixing estimates from heat flux measurements, The Natural Stratosphere of 1974, CIAP Monograph 1, DOT-TST-75-51, pp. 8-90 to 8-92.
7. Woods, J.D. (1968) Wave-induced shear instability in the summer thermocline, J. Fluid Mech. 32:791-800.
8. Woods, J.D. and Wiley, R.L. (1972) Billow turbulence and ocean micro-structure, Deep Sea Research and Oceanic Abst. 19:87-121.
9. Mantia, M.T. and Pepin, T.J. (1971) Vertical temperature structure of the free atmosphere at mesoscale, J. Geophys. Res. 20:8621-8628.
10. Carrier, G.F. and Pearson, C.E. (1976) Partial Differential Equations, Academic Press, Inc.
11. Spiegel, M.R. (1966) Theory and Problems of Laplace Transforms, Schaum Publishing Co.
12. Abramowitz, M. and Stegun, I.A. (1964) Handbook of Mathematical Functions, N.B.S. Appl. Math. Series #55.
13. Barat, J. (1975) Etude Experimentale de la Structure du Champ de Turbulence dans la Moyenne Stratosphere, C.R. Acad. Sc. Paris, 280, Ser. B, pp. 819-893.



14. Browning, K. A. (1967) Structure of the atmosphere in the vicinity of large amplitude Kelvin-Helmholtz billows, Roy. Met. Soc. Quart. J. 97:283-299.

## Appendix

### Continuous Estimate of Amount of Material Per Unit Area Passing Through Bottom of "Slab" Due to an Average Mixing Event and Modification of the Estimate of $K_B$ -CALC

Let the bottom of the slab be located at  $Z = Z_B$ . Let  $Z_0$  designate the center of a mixing layer, and we shall assume that the layer overlaps the location of  $Z_B$ . The latter condition, where  $\Lambda$  is the thickness of the mixing layer, is

$$2|Z_0 - Z_B| < \Lambda \quad (A1)$$

Let  $H(Z_0)$  be the height by which the mixing layer extends above  $Z_B$ . Then

$$H(Z_0) = \left[ \left( \frac{\Lambda}{2} + Z_0 \right) - Z_B \right] \quad (A2)$$

Define  $M(Z_0)$  to be the amount of material per unit area which passes through the  $Z = Z_B$  boundary as a result of mixing. Then

$$M(Z_0) = M_i(Z_0) - M_f(Z_0) \quad (A3)$$

where  $M_i$  is defined as the initial amount of material per unit area in the part of the layer which is above  $Z_B$ , and  $M_f$  is this amount after the mixing.

Assuming, as in the text, that  $\phi(Z)$  is linear and, for convenience,

$$\phi(Z) = a Z \quad (A4)$$

where  $a$  is constant, we have (using  $a = \partial\phi/\partial z$ )

$$M_i(Z_o) = (\text{height of layer above } Z_B) \times (\text{average initial concentration})$$

$$= H(Z_o) \frac{\int_{Z_B}^{Z_B+H} \left( \frac{\partial\phi}{\partial z} \cdot z \right) dz}{H(Z_o)} \quad (A5)$$

Similarly

$$M_f(Z_o) = (\text{height of layer above } Z_B) \times (\text{average final concentration})$$

$$= H(Z_o) \frac{\int_{Z_o - \frac{\Lambda}{2}}^{Z_o + \frac{\Lambda}{2}} \left( \frac{\partial\phi}{\partial z} \cdot z \right) dz}{(\Lambda)} \quad (A6)$$

When  $M(Z_o)$  is averaged over all possibilities consistent with Eq. (A1), we have

$$\overline{M(Z_o)} = \frac{1}{\Lambda} \int_{Z_B - \frac{\Lambda}{2}}^{Z_B + \frac{\Lambda}{2}} (M_i(Z_o) - M_f(Z_o)) dz_o \quad (A7)$$

After the calculations are carried out,

$$\overline{M(Z_o)} = \frac{\Lambda^2}{12} \cdot \left( \frac{\partial\phi}{\partial z} \right)^* \quad (A8)^*$$

---

\*This result was first obtained by T. VanZandt (private communication).

The estimate of  $K_B$  given as Eq. (4) in the text would thus be changed somewhat. Given that  $\Delta t_b = t_f/P^*$ , and identifying the flux  $\bar{F}$  in Eq. (3) with

$$\bar{F} = \frac{M(Z_0)}{\Delta t_b} \quad (A9)$$

thus, we obtain the new estimate:

$$K_B = \frac{(\Delta^2/4)P^*}{3\Delta t_f} \quad (A10)$$

This differs from Eq. (4) by a factor of 2/3 but, in spite of the agreement between the simulations and Eq. (4), Eq. (A10) would be theoretically more accurate than Eq. (4).<sup>†</sup> Equation (A10) is presumably the correct estimate to use in future analysis of experimental data along these lines; however, no explanation is available at present as to why Eq. (A10) does not agree with the simulations, whereas Eq. (4) of the text does. A 5-point numerical, finite-difference formulation of this appendix was carried out and the result was essentially identical to Eq. (A8). This remains to be clarified.

---

<sup>†</sup>Equation (4) was derived by using  $M(Z_0) = 0$  (see Rosenberg and Dewan<sup>1</sup>). This means that, instead of a "mix through" process, there was a "dump through" process.